UNIVERSIDADE DE LISBOA

FACULDADE DE CIÊNCIAS

DEPARTAMENTO DE ENGENHARIA GEOGRÁFICA, GEOFÍSICA E ENERGIA

Development of an ammonia portable low-cost air quality station

Ana Margarida Santos Antunes

Mestrado Integrado em Engenharia da Energia e do Ambiente

Dissertação orientada por:
Prof. Dra. Carla Silva

2019

Acknowledgements

To my grandmother, Maria Cremilda Gomes Antunes. For all the love, all the hours, companionship, scoldings, laughs, tears, caresses, teasings. All the soups you made, all the laughs, all the care you had, all the candies and sweets (your Arroz Doce and Mousse will be passed on for generations). For the wise advices and your curiosity. For the songs you sang, for the stories you told and for your care when I was sick. Thank you for teaching me how to move around a kitchen and how to fight back in life. Thank you for all the nights and for wanting me near you. Thank you for our walks and our talks.

Thank you, for everything. You will always be loved.

Resumo

A deterioração da qualidade do ar é um problema cada vez mais significativo para a saúde humana e para o ambiente. Assim, a monitorização dos poluentes, seja em espaços interiores ou exteriores, é cada vez mais necessária, de forma a aumentar a consciencialização das populações e a potenciar a criação de medidas de mitigação eficazes.

As estações de qualidade do ar de referência têm uma densidade espacial muito reduzida (uma estação por cada 1299 km^2) devido aos seus elevados custos. Tendo isto em conta, o presente estudo visou estudar e desenvolver uma estação de qualidade do ar de baixo custo, testando a sua validade e viabilidade. A estação em questão, a QAPT (acrónimo de Qualidade de Ar Para Todos), teve como objetivo a monitorização de amoníaco e outras variáveis secundárias (temperatura, T, e humidade relativa, HR), de forma a melhorar a performance do sensor de amoníaco e consequentemente do sistema num todo. O QAPT foi criado de forma a demonstrar a viabilidade do ponto que poderá pertencer, num futuro, a uma rede de monitorização da qualidade do ar de maior densidade espacial. A escolha do poluente a ser estudado, o amoníaco, adveio da necessidade de fazer uma melhor caracterização das concentrações e fontes emissores de amoníaco, uma vez que este poluente é monitorizado num número reduzido de estações de referência (ao contrário de poluentes mais conhecidos como o ozono ou partículas) e tem um elevado potencial de eutrofização e acidificação, sendo um importante precursor secundário de partículas.

Esta dissertação focou-se no estudo dos diversos sistemas da estação *low-cost* de qualidade do ar criada, nomeadamente, no sistema de amostragem de ar, no sistema eletrónico, no sistema de alimentação e no sistema de visualização e tratamento de dados. Assim, efetuou-se o estudo do comportamento e limitações dos diversos componentes da estação, verificando e estudando também os seus impactos no sistema como um todo. A validade da estação de baixo custo foi comprovada com a obtenção de resultados coerentes com a literatura existente aquando dos estudos do desempenho do QAPT em variados cenários, com particular ênfase na monitorização efetuada num salão de beleza e num armazém de criação de frangos. Aquando da monitorização no salão de beleza foi também possível verificar que as profissionais destes locais estão frequentemente expostas a muito elevadas concentrações de amoníaco, facto que é um perigo para a sua saúde. Os resultados obtidos na monitorização perto de estradas com muito tráfego e em cavalariças permitiu também mostrar um dos problemas mais recorrentes dos sensores de baixo custo: a falta de seletividade. No entanto há já variados estudos que se focaram na superação deste problema, sendo que os seus métodos poderão ser estudados em trabalhos futuros. Em termos económicos, a estação desenvolvida é muito satisfatória uma vez que custa apenas 133€ no seu estado atual. No entanto também se verificou que aquando futuras e eventuais melhorias, utilizando um Raspberry Pi de forma a fazer a comunicação para a *cloud* e ter mais espaço de memória, o protótipo fica a cerca de 165€, o que é muito satisfatório para uma estação de qualidade do ar. Não se aplicou a ligação à *cloud* uma vez que se verificou que esta punha em risco a portabilidade da estação pelo aumento do consumo de energia, o que inviabilizaria a autonomia do protótipo, baixando o seu tempo de monitorização de 28 horas para apenas 3 horas na melhor das hipóteses.

Neste trabalho foi também estudado o impacto da temperatura e humidade relativa no sensor *low-cost* de amoníaco (MQ137) que levou à criação de uma rotina (código de calibração com T e HR) de forma a minimizar o impacto de ambas as variáveis no sensor, tendo esta sido aplicada com sucesso. O sistema de amostragem desenvolvido minimiza as desvantagens de se terem colocado os sensores dentro de uma caixa, permitindo assim que o sistema funcione de forma satisfatória tanto em medições estáticas como em medições em movimento. Já na parte das ligações entre os componentes foi tida em conta a necessidade de minimizar o espaço ocupado e o peso do sistema, tal como a sua estabilidade, tendo para

isso sido feito um PCB. Em relação ao sistema de alimentação, das várias alternativas estudadas e tendo em conta os seus impactes no sistema (a nível térmico, das tensões impostas, capacidade, entre outros), verificou-se que a opção mais favorável é a utilização de um *power bank* solar. Por fim, verificou-se que a integração dos dados obtidos com um sistema de informação geográfica é de particular interesse quando aplicado às estações de qualidade do ar de baixo custo portáteis, facilitando a visualização espacial dos dados e consequentemente aumentando o potencial de consciencialização do sistema desenvolvido.

Palavras-Chave: estação de qualidade do ar, *low-cost*, portátil, sensor de amoníaco, sistema de amostragem

Abstract

Air pollution is becoming an ever-increasing problem for human health and the environment. As such, the monitorization of air pollutants, both indoors and outdoors, is increasingly necessary in order to enhance awareness and the creation of more effective mitigation measures.

The existing reference air quality stations have a very low spatial density due to their high costs. Considering this, the following study focused on the development and study of a low-cost air quality station, testing its validity and viability. The developed station, QAPT (which stands for Air Quality for All – "Qualidade de Ar Para Todos") focused on the monitorization of ammonia and other secondary variables to improve system performance, having been built as a proof-of-concept, as a node for a broader monitorization network of high spatial distribution. The monitorization of ammonia arose from the necessity to understand in greater detail the spatial disposition of ammonia emission sources, as this pollutant is monitored in very few stations (unlike better-known pollutants like ozone or particulate matter) and has a high eutrophication and acidification potential, as well as being a secondary precursor to particulate matter formation.

This work focused on the study of the several systems of a low-cost air quality station, particularly: air sampling system, electrical connections, power supply and data visualisation and treatment. As such, the limitations of the low-cost components and their behaviour in the system are studied in detail and discussed. The station's validity and viability, both in terms of the air quality monitorization (with consistent results from the low-cost MQ137 sensor) and total cost were assessed, laying the basic foundations for further work in the creation of nodes of a low-cost air-quality network of high spatial density.

The study assessed the impact of both temperature and humidity in the readings of the low-cost ammonia sensor (MQ137) and created a routine (calibration code) to minimise these effects, with proven success. The developed air sampling system minimises the limitations of having the sensors inside a case, thus allowing them to perform satisfyingly in both static and moving monitorization. The electrical connections were developed taking into consideration the need to ease trouble-solving and minimise volume and weight, with the creation of a PCB that allowed for greater system stability. Different power supply options and their impact on the system were studied, pointing to the advantages of using a solar power bank. Lastly, the integration of GIS software to analyse the data is proven to be of particular interest when applied to the low-cost air quality station data, improving the spatial visualisation of the data and thus enhancing the awareness potential of the system.

Keywords: air quality station, low-cost, portable, ammonia sensor, air sampling system

Table of Contents

List of Figures

List of Tables

List of Acronyms

2G	Second-generation cellular technology
ACGIH	American Conference of Governmental Industrial Hygienists
APA	Environmental Portuguese Agency
AQ	Air Quality
AQS	Air Quality Station
CCDR	Commissions for Regional Coordination and Development
EMEP	European Monitoring and Evaluation Program
Float	Floating-point number
GIS	Geographic Information System
GPRS	General Packet Radio Service
GSM	Global System for Mobile communications
I_2C	Inter-Integrated Circuit
IDE	Integrated Development Environment
INT	Integre
IPMA	Portuguese Institute of the Sea and Atmosphere
LCD	Liquid Crystal Display
LED	Light Emitting Diode
MOS	Metal-Oxide Sensors
NH_3	Ammonia
NH_4^+	Ammonium
NIOSH	National Institute for Occupational Safety and Health
NTC	Negative Temperature Coefficient
OSHA	Occupational Safety and Health Administration
PCB	Printed Circuit Board
PM	Particulate Matter
PM10	Atmospheric PM that has a diameter of fewer than 10 micrometres
PM2.5	Atmospheric PM that has a diameter of fewer than 2.5 micrometres
ppb	Parts per Billion
ppm	Parts per Million
QAPT	Qualidade de Ar Para Todos
R_0	Resistance of the MQ137 sensor in a 0 ammonia environment
RH	Relative Humidity
RH	Relative Humidity
R_s	Resistance of the MQ137 sensor
RTC	Real Time Clock

SD	Secure Digital
T	Temperature

1. Introduction

1.1. Framework

One of the major objectives of this dissertation is to pave a way to the democratisation of air quality information, through the creation and study of the building blocks for a low-cost AQ monitoring grid, of high spatial density. This grid network will, in turn, allow researchers to make a better characterisation of the pollutants emission sources and behaviour, allowing for the creation of more effective mitigation measures.

The local AQ issue is gathering more and more visibility and relevance in the European and global panorama due to its direct impact on human health. Since the effects of exposure to poor AQ are not directly noticeable for the most part, nor immediate, but are usually only visible in long-term scenarios being associated to various negative effects on human health, there is still a very real need for the increase of awareness of the populations to this problem. For this to happen, it is imperative to increase the access and acquisition of relevant data for better characterisation and monitoring of AQ and therefore for the society to take on a more active role in the mitigation of this issue.

Although the AQ issue is, nowadays, being taken more into consideration, this is not a recent problem for the European populations. With the appearance of dense housing aggregates in cities and an increase in car traffic and industry, this issue became critical in past decades, and Europe has already come a long way from the extreme situation it had in some of its major cities in the advent of the industrial revolution. For example, London has had, since the peak of the industrial revolution, many problems of poor air quality, associated with the industries pollutants emissions. These problems remained very critical until the end of the XX century, observable, for example, with the typical smog of the 50s and 60s decades [1]. The problems with the emissions of sooth and sulphur dioxide started to subside when the industry started using smaller and smaller amounts of coal in its operation, with the implementation of guidelines and laws for the regulation of pollutants emissions and with the ever-increasing deployment of renewables (characterised by lower local pollutants emissions). Other problems have arisen with the increased number of motor vehicles, for example, with an increase in the emission of small particles and nitrogen dioxide [1].

In China, with the atmospheric pollution from heavy industries, came extreme air quality problems that became so critical the government had to apply several different measures to decrease the pollutants emissions and the exposure of the population to it, with observed success [2]. Considering this, China increased the control on the industries emissions and announced stricter ambient air quality standards [3] and has been investing heavily in nuclear and in renewable energy such as hydro, wind and solar, and in natural gas power plants (that have the advantage of having lower emissions of particulate matter than conventional liquid fuels or coal) [4].

Adverse effects to human health have been extensively observed in populations living in places with low air quality [5], such as cancer, problems of the respiratory tract, heart diseases, fertility problems and even higher levels of psychological distress [6]. In fact, the knowledge of the real risk of living in lower air quality environments is still being assessed and improved, with recent studies suggesting that the number of deaths caused by air pollution in Europe might be more than twice the number of deaths accounted in former reports [7]. Thus, it is of great importance that countries commit to improving their air quality indexes, considering not only the human health and quality of life but also considering the added economic pressure and investment the treatment of these diseases entails and all the social repercussions these problems create in their respective societies.

There is still a long way to go in solving this issue, not only in the cities, with a needed decrease in particulate matter emissions and other pollutants, but also in the rural areas, with pollutant gases like ammonia, associated with the farming sector.

The pollutant gas being addressed in this dissertation is Ammonia (NH_3). The main emission sources of Ammonia are in the agriculture sector (particularly livestock production) and still lack a spacially detailed characterisation because this pollutant is not usually monitored in most air quality stations. The interest in monitoring this pollutant arises from the fact that it acts as a precursor to secondary inorganic aerosols and particulate matter (mainly PM2.5), which in turn are very harmful to human health and biodiversity. This pollutant also has a major role in the increasing problems of acidification and eutrophication, resultant from its dissociation and dispersion through the atmosphere. It can also react in the atmosphere, transforming to ammonium nitrate, which can then split, when at high temperatures and low altitudes, in nitric acid and ammonia. These can be quickly deposited on the earth's surface. This deposition acts as a fertiliser to some plants that are well adapted to a nitrogen-rich climate. Although this might look, at first sight, as a good outcome, the truth is that this is leading highly specialised flora that is adapted to low-nitrogen climates to wither. Besides, this also increases the problem of acidification of the soil and eutrophication of marine climates, also increasing nitrous oxide emissions [8]. In case of direct inhalation of gaseous ammonia (which usually only happens near the source of emission because ammonia is a short-lived chemical), the acute exposure guideline levels set by the U.S. Environmental Protection Agency for 8 hours of exposure are of 30 ppm for mild irritation, 110 ppm for acute irritation (eyes and respiratory tract) and 390 ppm being the threshold of lethality [9]. According to OSHA (Occupational Safety and Health Administration) [10], the exposure limit values are of 25 ppm for 8 hours and of 35 ppm for 10 minutes.

Considering the above mentioned, this dissertation will focus on the development of a portable, low-cost monitoring station, with the capability of building the basis module of a network for air pollutants characterisation, in this case focusing on ammonia.

1.2. Objectives

The objective of this dissertation is to study, build and test the viability and validity of a low-cost air quality monitoring station (AQS) that focuses on the monitoring of NH_3 (Ammonia). In addition, it monitors complementary variables that affect the quality of the acquired data, such as the ambient temperature (T) and relative humidity (RH). The AQS developed in this thesis is to be portable (for ease of transport and installation) and send the relevant data to an SD card to be articulated with a GIS program in order to have a spatial perspective of the distribution of emission sources. The idea of the developed AQS is to support in the future other air quality pollutants sensors, which can be used as nodes of an air quality monitoring network.

The study of the quality of the acquired data will focus on studying several phenomena associated with the normal functioning of the systems, such as the existence of electromagnetic, physical or chemical interferences or the warm-up time of the system. The developed AQS will be tested in six types of environments: a supposedly zero NH_3 environment, air salon environment with hair dyes, public toilets, horse stable yard, near busy roads and in a poultry farm. This will allow testing the AQS sensitivity to different environments. Lastly, this thesis will study the response of the built system and the influence of the air movement in the normal functioning of the prototype (for example, on-road vehicles).

1.3. Structure of The Thesis

The present dissertation has six main chapters, starting with the necessary surrounding framework and going through the several stages of the conceptualization, assembly and testing of the low-cost air quality station named QAPT (which stands for “Quality of Air For All” or in portuguese “Qualidade de Ar Para Todos”), ending with a note of recommendations for future improvements and with the code, that is the backbone of QAPT, in the appendix.

2. Literature Review

2.1. Research Variables

2.1.1. Ammonia

Being one of the most important nitrogen species in the atmosphere, besides N_2, ammonia (NH_3) is emitted in gaseous form and has a low residence time (thus only found near the emission sources). It is readily transformed in fine particulate NH_4^+ salts by reacting with acidic substances such as sulfuric acid, nitric acid, nitrous acid, and hydrochloric acid. The fine particulate ammonium sulphate [$(NH_4)_2SO_4$] and ammonium nitrate [NH_4NO_3] have prolonged atmospheric residence times (approx. 6 days) and can be transported to very large distances (thousands of kilometres) [11]. In fact, several studies in Chinese and northern European cities show the real impact of this transport in urban air quality, having studied smog episodes related to far away agricultural enterprises from the North China Plain (in the case of Beijing [12]) and rises in particulate matter in some cities in Sweden [13] derived from neighbouring countries such as Germany and Poland. The large residence time and dispersion of the fine particulate ammonium salts allied to the fact that these fine particles are of very small dimension (PM2.5 and PM10) makes this an ever-increasing transboundary problem. As such, many countries have signed treaties and protocols like the Guthenberg protocol, in order to limit their national emission quotas for transboundary pollutants. Portugal has also adhered to this protocol, making its own limits (National Emission Ceilings) and to the Convention on Long-Range Transboundary Air Pollution, complying with the EMEP program (European Monitoring and Evaluation Program).

NH_3 is mainly emitted by the agricultural sector (with the use of N rich fertilizers), animal feedlot undertakings (volatilization from animal waste) and biomass burning (ex: forest fires, which have been a recurrent problem in Portugal in the past years). This fact makes it very difficult to diminish ammonia emissions due to the need to grow more and more food to support the exponential growth of the human population; as so, ammonia emissions have been slowly increasing in the past six years [14], as shown in Figure 1. Together, these emission sources account on average for 80% to 99% of ammonia emissions in Europe [15]. Therefore, most of the studies of ammonia emissions are focused in rural areas, making the study of other areas necessary for a better understanding of the current panorama. Other emission sources are also known, even though at a much smaller scale, such as road traffic (because of the ammonia slip and poor combustion on automotive Otto cycle engines), industries and human waste (volatilization). In fact, recent studies show that the role of road traffic NH_3 emissions in cities is more significative than previously assumed. Such has been demonstrated in several megacities in China [12] [16]. For example, in Shanghai, it was estimated that vehicle emissions contributed with 12.6% to 24.6% of the atmospheric ammonia in the urban area and between 3.8% and 7.5% for the whole Shanghai area. Interestingly, another source that might have more influence than previously assumed is the human waste, particularly biological sources like garbage containers and wastewater or solid waste treatment plants, as observed in Barcelona, particularly in more densely populated areas with a dense urban architecture that attenuates air recirculation [17].

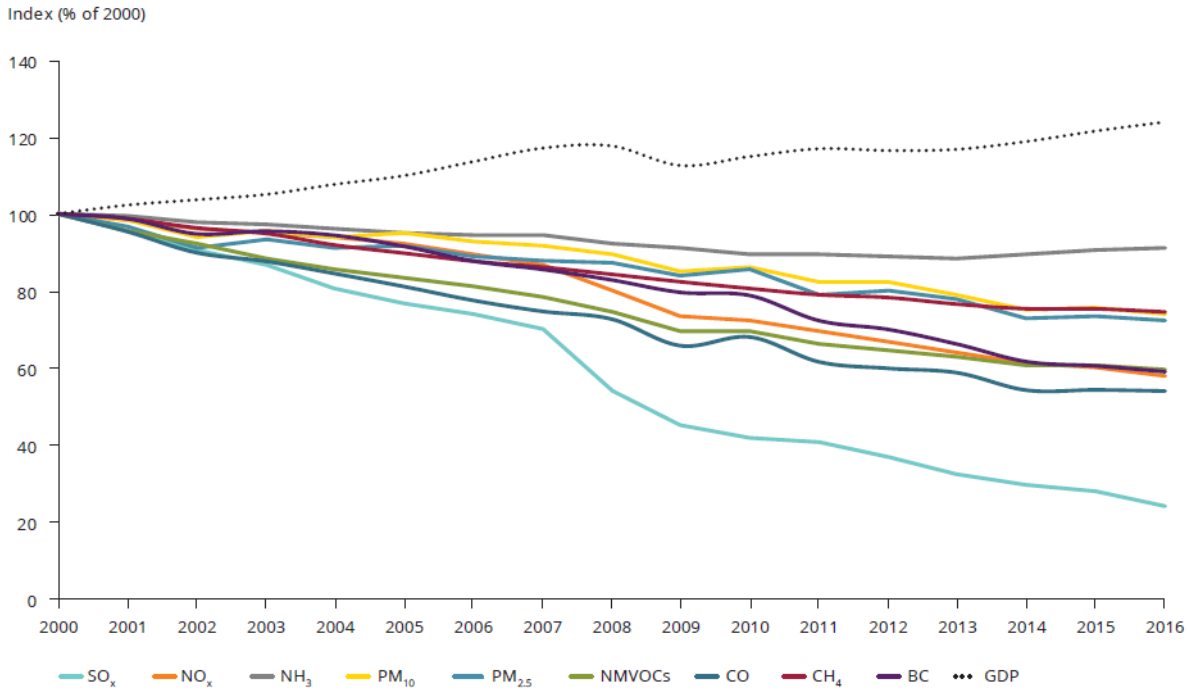

Figure 1- Development in EU-28 emissions, 2000-2016 (% of 2000 levels) – reproduced from [14]

The impact of ammonia emissions does not stop at being a health hazard because of the inhalation of fine particles of ammonium salts or at irritating the respiratory tract when inhaled directly, but instead, it also has a huge eutrophication and acidification potential. Both the ammonium sulphate and ammonium nitrate release the ammonium ion when they are deposited in the soil, forming a small amount of acid. This reduces de pH of soil and water and ultimately leads do acidification, which harms both plant and animal life [14]. The ammonium ion will also cause eutrophication because of the excess deposition of nutrient nitrogen, which will aggravate a situation that is already critical, since EMEP estimated that the limits for eutrophication (critical loads) were exceeded in the vast majority of the European countries, with more than 61% of the European area in this situation [14].

For all the factors mentioned above, it becomes of imperative importance to reduce ammonia emissions. This reduction can be facilitated by investing in further studies, planning and characterising the emission sources and their behaviour. Some works already pave this way: a recent study [18] suggests that the most efficient season to diminish NH_3 emissions in order to attenuate their effects is, surprisingly, in winter, when there are naturally fewer emissions (due to a lesser deployment of fertilisers than in summer) and less volatilisation (because of lower temperatures). Considering this, the most effective reduction should happen in the agricultural sector, since it is responsible for the biggest share of emissions in winter. This study also found that by applying this and other methods to reduce ammonia to half of its actual emissions, the total amount of PM2.5 could be reduced to ¾ of its value, which would be a tremendous improvement in air quality. In the path to a better characterisation of emission sources, a biological option is being studied: the use of nitrophytic and nitrophylic lichens to monitor the spatial distribution of ammonia sources, with confirmed application [19].

2.1.2. Temperature and Relative Humidity

These parameters affect the human levels of comfort, food supplies and many other aspects of life directly and, as such, have been subject to interest since the dawn of civilisation. The interest of this study comes in their direct impact on the measurements of ammonia concentration, because of the sensibility of the sensor to temperature and relative humidity variations. This sensibility is due to the variation of the internal resistance (R_s) with both parameters and the respective change in calculated ammonia concentration. This dependency can be shown in Figure 2, from the sensor's datasheet [20]. It is easily observed in the figure that small variations in temperature and humidity can lead to huge alterations of the sensor's values, being more accentuated with from -10 to 20℃.

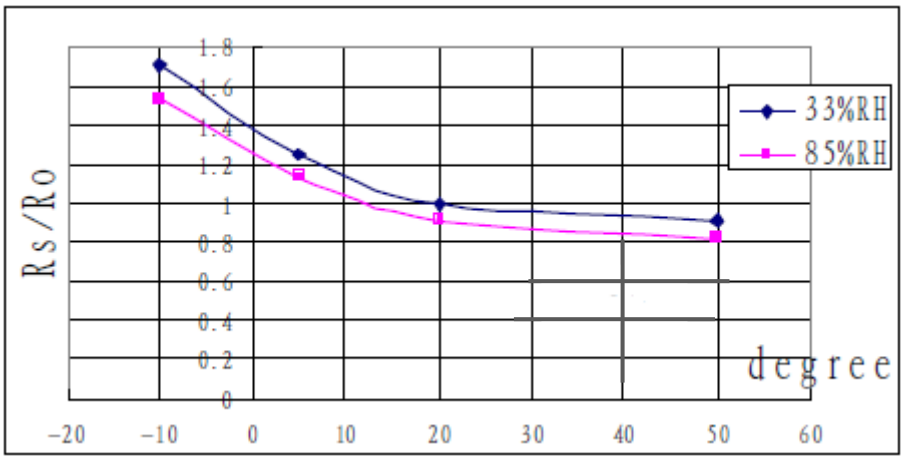

Figure 2 - Typical dependence of the MQ137 on T and RH [20]

2.2. Existing AQS

It is considered in this context, as a simplification, that there are nowadays three main types of air quality stations: gadget like stations, small stations, and reference stations.

The **gadget like stations** are portable, having been recently introduced in the markets. They are very small and lightweight, which facilitates their transport. Their cost is very low (usually bellow 200€), and their small size allows them to be transported by anyone in their quotidian. Many have built-in *apps* in order to visualise the data in real-time, but the measured data is usually of qualitative order because of the low accuracy of the sensors. These usually measure only one type of pollutant but are a good step in fomenting a rise in the awareness of the population concerning air quality. Examples of these stations are the British company CleanSpace [21] and the North-American AtmoTube [22].

Another type of stations are the so-called **small stations**, such as the station being built and studied in this dissertation. These are portable, and usually, have lesser mobility than those of the first type mentioned above. They also have more accurate sensors and usually measure several pollutants (2 or 3 pollutants concentrations in ppm or ppb). Since these stations are portable and much less expensive than the reference stations (below 2000€, although the objective in this thesis is to be even lower, below 200€), these allow a much larger area of implementation, with higher data collection spatial density. They present some challenges, such as the need for more regular calibrations of the sensors (because of

their much larger drift), the needed adjustments to cope with the interference of other pollutants or even of electronic "noise" (electromagnetic interferences). An example of this type of stations are the Decentlab [23] stations.

Lastly, the **air quality reference stations** are usually implemented at a national or governmental level (*ex.*: in Portugal the monitorization is done with reference stations from APA and IPMA – Environmental Portuguese Agency [24] and Portuguese Institute of the Sea and Atmosphere, respectively), being organized in large networks of very low spatial density, see Figure 3 [25]. This low spatial density is mainly due to the fact that these systems are very expensive (usually far more expensive than 20 000€ because of the use of complex instrumentation) and of very large size and weight, also making them impossible to be portable. These stations produce data of very high reliability and accuracy. They measure many pollutants of interest to the human health and climate, although some of the less-studied pollutants, like ammonia, are usually not in the scope of these stations. Most of the air quality monitoring reference stations in Portugal are from APA (71 stations in total [26]), and only a few are rural stations. The spatial dispersion of the existing monitoring network is so big that there is only one station for every 1299 km^2 at a national level. The spatial distribution of the stations is not homogeneous, being concentrated in the two main CCDR [27]: Lisboa e Vale do Tejo (with one station for every 452 km^2) and Norte (with one station for every 887 km^2). Of this network, only two (in Alfragide and Monte Velho), that belong to the AirBase network, are nowadays monitoring ammonium in PM2.5 and PM10 and reporting to EEA (European Environment Agency). Their available online data of ammonia measurements is flawed, being inexistent for the last eight years, excluding one value for one hour of the year 2016 in which they supposedly measured 2.44×10^{-4} ppm and 1.58×10^{-4} ppm, respectively. IPMA, in charge of the EMEP stations in Portugal, has only three EMEP rural background stations, of which at least one monitors atmospheric ammonia along with other pollutants. The situation of ammonia monitorization in Portugal, which seems already poor given the low number of stations monitoring ammonia, is aggravated because IPMA does not possess enough qualified personnel to correctly monitor the few EMEP stations it has [28].

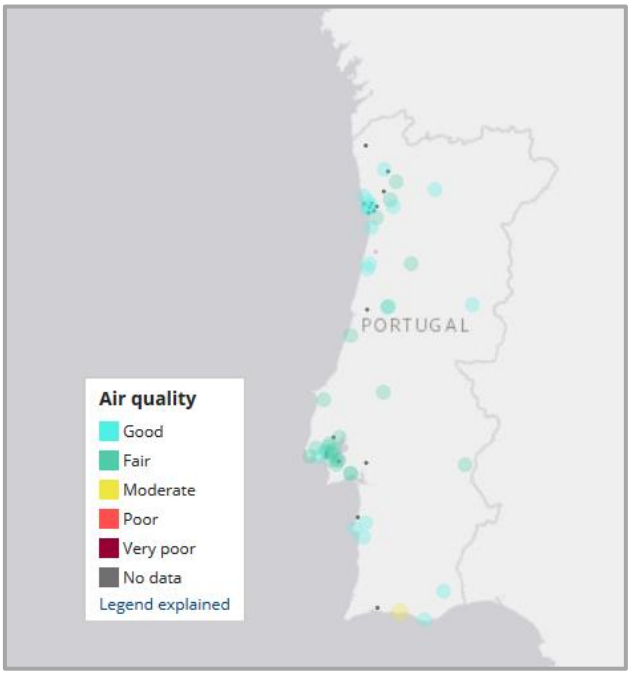

Figure 3 - APA Reference Air Quality Stations in Portugal [25]

The stations that measure NH_3 are rural background stations and they usually measure ammonia concentrations in $\mu g/m^3$. According to [29], the maximum value measured in these stations was of less than 10 $\mu g/m^3$ between 2013 and 2014, which is equivalent to 0.0141 ppm of NH_3, whilst the minimum value was of 0.20 $\mu g/m^3$, which is equivalent to 2.27×10^{-4} ppm of NH_3. These values are much lower than those measured by the QAPT station, due to the short lifetime of ammonia in the outdoor environment. Therefore, the station is best suited to measure indoor ammonia concentrations or outdoor concentrations very near emission sources, being more useful to identify emission sources than to do static monitoring of ammonia concentrations at a national level.

Regarding indoor environments, the limits are:

Table 2.1 - NH3 concentration limits and effects, adapted from [9], [30] and [31]

Concentration	*Evidence*
< 25 ppm	People notice the presence of ammonia at 1ppm
25 ppm for 8 hours	NIOSH's Time-weighted average limit
35 ppm for 15 minutes	NIOSH's and ACGIH's short-term exposure limit
50 ppm for 8 hours	Current OSHA's time-weighted average permissible exposure limit
80 ppm from 30 minutes to 2 hours	NCBI: moderate to highly intense irritation

As such, the QAPT can be used in the monitorization of these limits as its range is from 5 ppm to 200 ppm of ammonia.

3. Methodology

This chapter will focus on the explanation of the several steps and procedures implemented during the course of this thesis. For a brief exposition on the followed methodology, consult Annexe B.

3.1. Component Selection and Operation

In this section, a comparison is presented of various available options for the QAPT subsystems (sensors, air intake, wiring, data presentation) and the selection process of the used devices is explained.

3.1.1. NH_3 Sensor

There is a wide option of techniques for NH_3 detection, but most belong to three main categories: solid-state sensing methods, optical methods and other methods [10] as can be seen in Figure 4. The sensing method used in the air quality system studied falls under the first category, with the use of a metal-oxide based sensor (MOS).

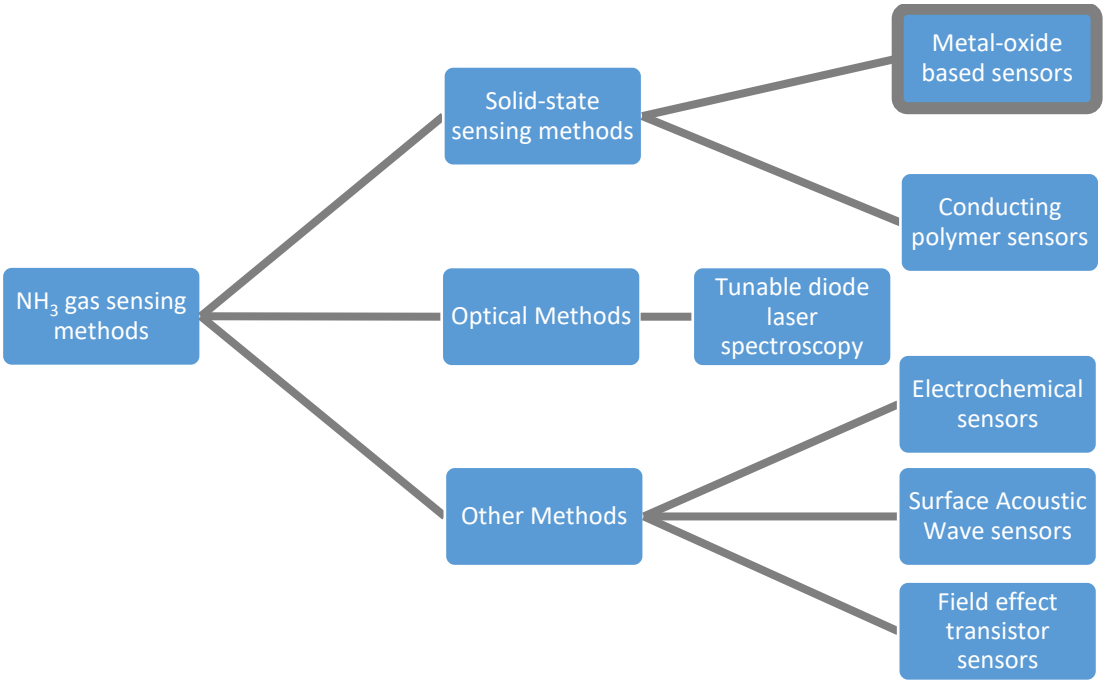

Figure 4 - NH_3 sensing methods and techniques - reproduced from [10]

The MOS have been mass-produced because of their low cost, robustness, and flexibility in fabrication. The most widely used metal oxides used for NH_3 detection are SnO_2, ZnO, TiO_2 and MoO_3 [10]. These sensors rely on changes in the semiconductor's conductance when exposed to reducing gases like ammonia. Unfortunately, these use high temperatures and lack enhanced selectivity and as such, it may be sensitive to other reducing gases, therefore creating “false positives” in their presence [32]. This problem can be attenuated by controlling the range of temperatures at which the sensor is working, by

creating alloys with the metal-oxides and noble metals or by adding structures of nanocomposites to the top layer of the metal-oxides, enhancing sensing performance towards NH_3.

The sensor used in this work is the $MQ137$ (see Figure 5) which uses SnO_2 as semiconductor. This is a non-transition-metal oxide. Its work is based on redox reactions between the surface of the metal and the measured gas. The molecules of O^- react with the gas and alter the resistance of the sensor (R_s), which in turn results in a change in the voltage between the analogue signal and the ground pin (see electric scheme in Figure 6).

Figure 5 - MQ137 Ammonia Sensor Module

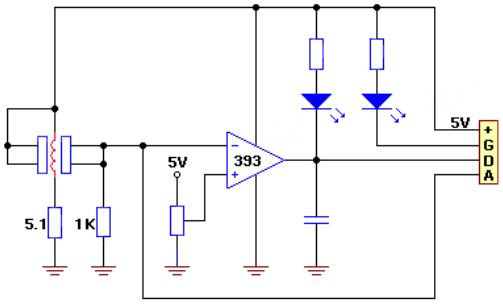

Figure 6 - Electric Scheme of MQ sensors modules

The MQ137 sensor was chosen for its good price-quality ratio, getting reasonable measurements with a small initial investment. A very sturdy sensor that is easily and affordably accessible (easier to replace when needed), the MQ137 is also Arduino compatible (analogue output), which was another reason for its choice. Besides, by developing the connections to this sensor, QAPTs use can be easily extended to other sensors of the MQ sensor family, allowing it to measure various other air pollutants, which makes the QAPT a possible universal air quality monitoring system, being an important feature of the developed system. This sensor can measure ammonia concentrations from 5 to 200 ppm. These concentrations are quite high when compared to those measured in reference air quality stations, as was mentioned in sub-chapter 2.2. As such, it is evident that this sensor is best suited for indoor measurements and characterisation of emission sources (that naturally present much higher concentrations of ammonia), such as industry or poultry farms.

3.1.2. Development Board

The Arduino Uno is an Italian microcontroller development board based on the ATmega328P that is open-source and prototype oriented. With 14 digital pins and six analogue pins, this small board is capable of running a simple program (always one at a time) written in its own editor, the Arduino IDE, in the LUA programming language, that is somewhat similar to the C language. This board has a relatively slow Clock (16MHz) and supports I2C and SPI protocols. It can be powered directly from a computer USB port, from an external power source by a DC jack or by the Vin pin.

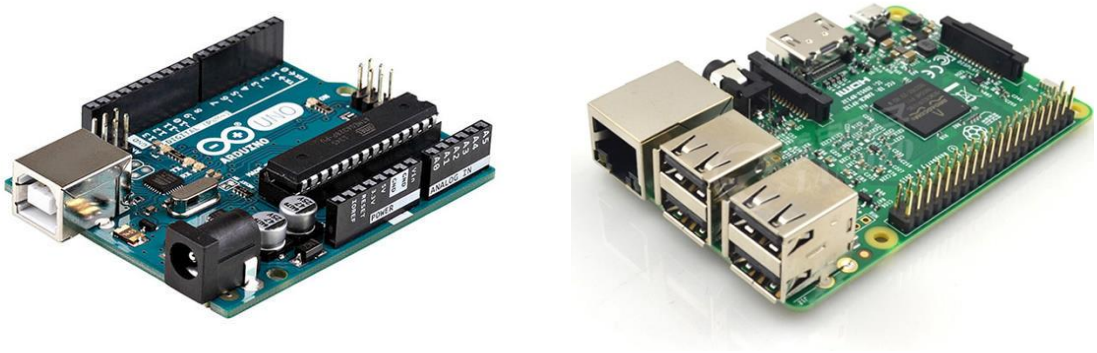

Figure 7 - Arduino Uno vs Raspberry Pi 3b

In order to control and assemble the core of the air quality station, there were two main options: using an Arduino board or a Raspberry Pi board (see Figure 7); both have a huge online community, are very flexible and good for prototyping, and are low-cost development boards. As such, the choice consisted of a matter of doing the most with the simplest, most inexpensive and less energy-consuming board, thus distinguishing the Arduino board as the most adequate for the purpose, concretely the Arduino Uno board. Although the Raspberry had a much higher processing capability and memory than the Arduino, this was not considered as a limiting factor because the air quality station was not expected to do many or complex computations, enough for a microcontroller to handle easily. Because of the portability of the station, energy consumption was an important factor to consider and as such, having a much lower consumption made the Arduino Uno the most interesting option. As such, the chosen development board was the Arduino Uno microcontroller, which was also more affordable than the Raspberry Pi board.

3.1.3. Temperature and Relative Humidity Sensor

The studied sensors have two separate systems for the measurement of temperature and relative humidity: one capacitive humidity sensor and one thermistor. The thermistor of these sensors is an NTC thermistor, which is a resistor whose resistance is highly dependent on temperature, decreasing when the temperature rises [33]. The capacitive humidity sensor consists of a hygroscopic dielectric material (a thin film of plastic or non-conductive polymer) placed in the middle of a pair of electrodes [34]. The voltage changes when the moisture is attracted to the film and makes contact with the electrodes. This change in voltage can then be converted into a digital reading of the amount of moisture in the air.

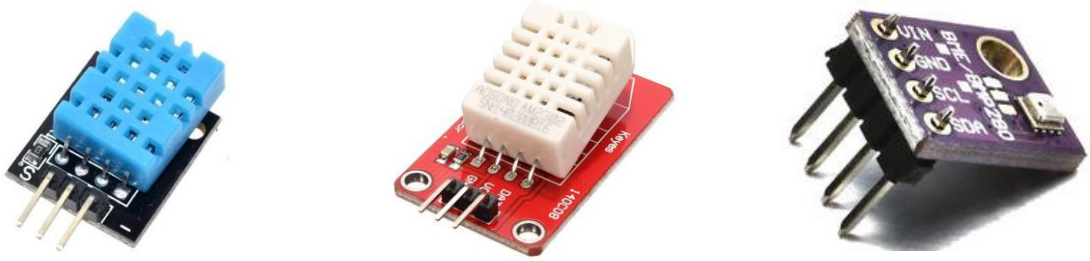

Figure 8 - T and RH Sensors; DHT11, DHT22 and BME280 in presentation order

In order to measure the temperature and relative humidity, there were three main options: the **DHT11** sensor, the **DHT22** sensor, and the **BME280** sensor (**see** Figure 8**)**. The two first ones differed mainly in the response speed and slightly in the accuracy, a factor that, at first, pointed at a superiority of the DHT22 over the DHT11. Even so, being both very popular amongst the online maker community and costing approximately the same, they were both considered of interest to the subsequent studies. The BME280 had more supporters in the online maker community and not only measured temperature and relative humidity but also the atmospheric pressure, ergo also the approximate altitude, and was in the same price range as the other two sensors. As such, this was, from the beginning, considered the most promising sensor.

In order to establish which was the most appropriate sensor for the QAPT AQS, a comparison experiment was undertaken: 2 sensors of each sensors family (2 DHT11, 2 DHT22 and 2 BME280) and one reference sensor (GE Telaire 7001) monitored, for a period of 3 days, the ambient temperature and relative humidity and proceeded to the respective data logging.

The Telaire sensor had its own separate data logging system and as such, no additional connections were needed besides the connection to a computer. In order to do the data logging of the remaining sensors data, an SD card module was connected to the Arduino and the corresponding code was written in the Arduino IDE. This code occupied more of the microprocessors storage than expected, making the system unstable and as such, the code was subject to several stages of optimisation for the problem to be solved. These optimizations were mainly simplifications of mathematical functions (ex: using power function instead of logarithmic function), of the monitored data storage usage (ex: treating data as *ints* instead of *floats*) and reduction of the number of "heavy" storage usage functions (ex: reduction of the number of *strings* used in the code). For the connection and communication of the BME280 sensors with the microcontroller, the need for an I_2C multiplexer arose and as such this element was introduced in the systems circuits configuration.

Another requirement for the data logging was the use of an RTC in order to have the timestamps associated with the measured data and be able to compare the data of the different sensors. The measurements were performed with a set interval of 1 minute, which was considered a reasonable interval taking into account the temperature and relative humidity velocity of variation in the enclosed environment being monitored. This experiment was conducted from 13 of April to 16 of April 2019.

The acquired data from the six sensors being tested was linearly interpolated in order to be compared with the reference sensor as the measurement interval had some lag derived from the Arduino processing. The small lag distributed across the monitoring interval acquired a larger significance (total of 42 seconds difference in the end) and had to be addressed.

The final wiring diagram of the experiment can be seen in Figure 9 and the reference sensor and datalogger in Figure 10, respectively.

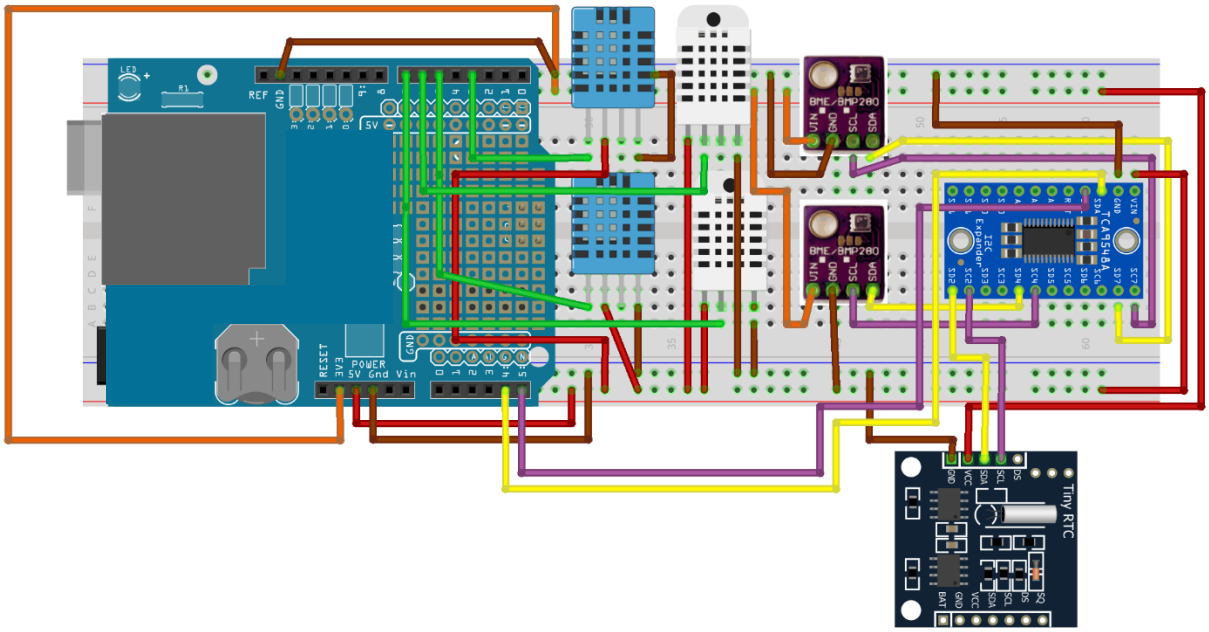

Figure 9 - T and RH experiment wiring diagram made on *Fritzing*

Figure 10 - Telaire 7001 sensor kit

3.1.4. Real-Time Clock

A real-time clock (RTC) is an inexpensive integrated circuit that keeps the time and date updated, being usually found in most computers and servers. Much like an everyday wristwatch, the RTC maintains track of time by counting the cycles of an oscillator – a piezoelectric crystal – usually quartz. This information is then transmitted to a microprocessor by an SPI or I2c serial bus and can be readily converted to time, date, day of the week, day of the month or even gap years.

One of the essential features of this integrated circuit is its ultra-low power consumption. This allows the circuit to run with only a coin battery for long periods of time and gives it autonomy from the power

source of the main circuit, allowing the RTC to keep running with the updated time and date even when and after the main circuit is turned off.

The RTC module used in the AQS in study is the Tiny RTC (see Figure 11), which is based on the clock chip DS1307 that communicates with the I2C protocol.

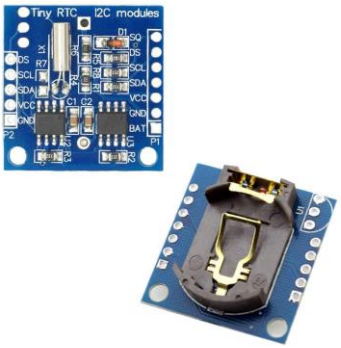

Figure 11 - Tiny RTC module back and front views

Initially, the RTC used in the AQS was a DS1302 RTC module. This module, acquired online, was used in the first experiments and presented stability problems, such as stopping for a little time and then continuing. This led to the acquisition of another RTC, the DS1307 Tiny RTC module. This new module did not present problems and needed less Arduino pins because it communicated through I_2C protocol and was connected to the TCA9548A I2C multiplexer breakout board.

3.1.5. I2C Multiplexer Breakout Board

An I2C multiplexer breakout board is an integrated circuit that allows a microprocessor to communicate with several same-address I2C devices. These breakout boards have multiple I2C addresses (multiple SDA and SCL pins) that can mask the original I2C address of the connected devices, allowing for a clear communication between the microprocessor and, for example, several sensors of the same family. Besides, when using microprocessors with limited I2C compatible pins (the Arduino Uno has 2 SDA pins and 2 SCL), this board increases the amount of I2C devices one can connect to the microprocessor.

The multiplexer used in this dissertation is the TCA9548A (see Figure 12), which has eight different I2C addresses.

Figure 12 - TCA9548A I2C multiplexer breakout board

3.1.6. Micro Diaphragm gas pump

A micro gas pump is a pump of very small dimensions that is built to work with a small flow rate of gas - in this case, a small flow rate of air. The most common types of pumps for this small size and flow rates are diaphragm pumps, peristaltic pumps, and linear pumps. These micro pumps are lightweight, which is an important factor in systems of reduced dimensions. The micro diaphragm gas pump does not need lubricants and as such, it has a contamination-free pumping. This kind of pumps is more resistant to corrosion than other pumps (important because the air samples might have considerable amounts of corrosive fluids) and has a long service life.

Diaphragm pumps use pressure or vacuum to transfer the fluid between the inlet and outlet valves. This pressure/vacuum is created by the upwards and downwards movement of a diaphragm (see Figure 13) that is clamped to an eccentric connection rod, connected to the axis of a dc motor.

The micro eccentric diaphragm gas pump used in the AQS in study is an RS D series pump (see Figure 14 - RS D series pump) with an adjustable flow rate that can be controlled with a simple difference in the voltage applied to the pumps terminals (input voltage from 3V to 4.5V). It is of small size and weight, which is important for the portability of the whole system.

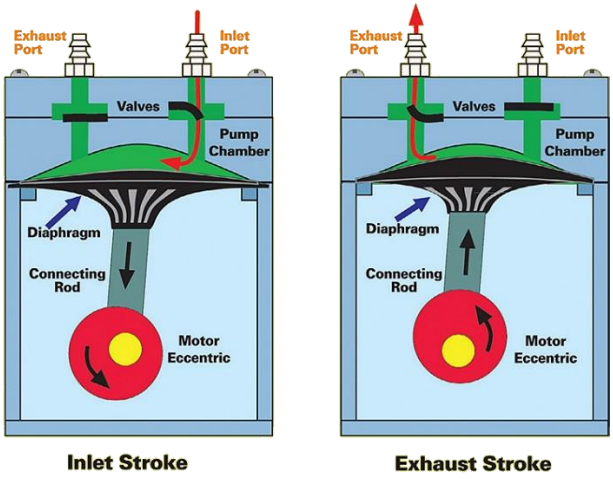

Figure 13 - Internal mechanisms of a diaphragm pump – reproduced from [35]

Figure 14 - RS D series pump

In its initial configuration, the air sampling system was not separated from the electrical system, and the air inlet was made through inlet fins and the use of a fan. This caused some problems to arise: the heat from the circuitry would heat up the enclosed air and as such, the temperature would rise and the relative humidity would fall. The study of the distribution of the system's temperature was made by conducting a series of infrared thermographies to the QAPT's interior, for the different types of power connections, as can be consulted in annexe D. It was also impossible to change the flow of air being analysed. As an improvement, the two systems were separated by making use of a micro diaphragm gas pump. Therefore, the system became capable of sampling the outside air having accurate outside air temperature and humidity measurements, also becoming able of, if needed, varying the sampling flow, by changing the voltage at the terminals of the pump, for example by using a digital potentiometer (of interest to maintain the isokinetism of the flow in moving measurements in future works). Besides, the pump also had the advantage of being able to extract air without the risk of having lubricants interfering

with the measurements of the analysed air samples. The air sampling system diagram, which can be seen in Figure 15, shows that the air goes first through the temperature and relative humidity sensor and only after that through the ammonia sensor. This order was implemented since the ammonia sensor has a resistance that dissipates heat and it would otherwise interfere with the measurements of the temperature and relative humidity sensor.

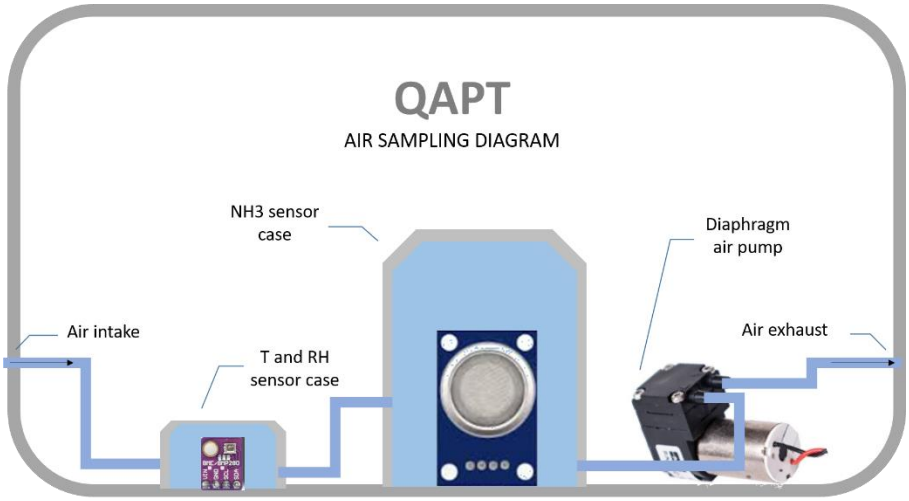

Figure 15 - QAPTs air sampling diagram

3.1.7. Visual interface

In order for the user of the AQS to interpret with ease and have real-time access to the most relevant measured data, two systems were installed: an LCD and an RGB LED. The LCD communicates with the microcontroller through the I2C protocol. The installed LCD (see Figure 16) allows writing digits in two rows and sixteen columns, which is enough to write some initial indications of the AQS status and other relevant data. The RGB LED has the ability to give a qualitative character to the information by adjusting its colour with the concentration of ammonia.

Figure 16 - 16*2 I2C LCD

Figure 17 - RGB LED for visual cues

3.2. Sensor Tuning and Calibration

3.2.1. MQ137

For the lack of a reference NH_3 sensor, the calibration procedure followed in this work was the application of the factory parameters. This mathematical method of calibration has inherent errors because the factory results are for a generalised conception of the MQ137 family sensors in very restrict testing environments. As such, given that each sensor should be individually calibrated for its own errors, this procedure will have some limitations.

The MQ137 sensor, being an analogue sensor, had to have its output (analogue variation in the Arduino pin) converted to meaningful variables. As such, firstly the output had to be converted to a voltage variation with (3.1),

$$MQ137\ voltage_{output} = analog_{output} \times \left(\frac{5}{1023}\right) \tag{3.1}$$

and, with equation (3.2), to a physical variable, the R_s, which is the resistence of the sensor when exposed to a certain amount of NH_3.

$$R_s = \frac{5 \times R_L}{MQ137\ voltage_{output}} - R_L \text{ in } k\Omega \tag{3.2}$$

Where R_L is the resistance load of the MQ137 module, in this case, 1 $k\Omega$.

The baseload resistance (R_0) of the sensor had to be known to calculate the concentration of ammonia. For this, the sensor had to be heating two days in a row in a 0 ammonia environment in order to calculate the R_0 with the R_0 code in annexe, through a series of monitoring loops to average the R_0 value. Knowing R_0, it was then possible to calculate the concentration of the gas (in this case NH_3 in ppm) by following the equation that depends on the R_s/R_0 ratio, which was deduced from the sensors datasheet graphic in Figure 18.

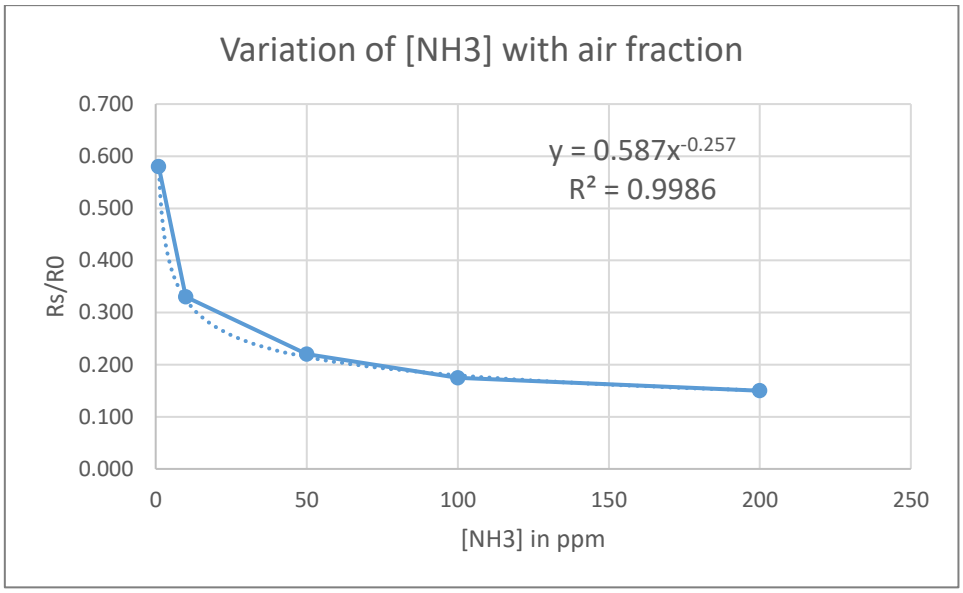

Figure 18 - Typical sensitivity characteristic of the MQ137 to NH_3 – reproduced from [36]

The equation obtained from the power regression was a good fit to the points taken from the datasheet ($R^2 = 0.9986$) and so, solving for the concentration of ammonia, equation (3.3) was used in the code, as can be seen in annexe.

$$[NH_3] = \left(\frac{\left[\frac{R_S}{R_0}\right]}{0.587}\right)^{-\frac{1}{0.257}} \; in\ ppm \tag{3.3}$$

The MQ137 sensors are extremely dependent on temperature and relative humidity variations, a factor that led to their monitorization in the station in order to attenuate the effect with data calibration.

This calibration was done by consulting the graphic in Figure 2 from the MQ137 datasheet [20] and plotting the data, finding the equations to the variation of R_s/R_0 with T and RH through second order polinomial interpolations. The routine written in the code in annexe was created using intervals of action (from 0 to 59% of RH and from 59% upwards) in order to follow one or another of the two possible equations (see equation (3.4) and (3.5) for the calibration with temperature and humidity (variation based on the 33%RH equation or the 85%RH equation).

$$\begin{cases} \dfrac{R_S}{R_{0_{33\%}}} = 0.0003T_1^2 - 0.0255T_1 + 1.4004 \;\; , \;\; if \;\; 0\% < RH < 59\% \\ \dfrac{R_S}{R_{0_{85\%}}} = 0.0003T_1^2 - 0.0231T_1 + 1.2808 \;\; , \;\; if \;\; RH \geq 59\% \end{cases} \tag{3.4}$$

$$\begin{cases} \frac{R_s}{R_0}calibrated_{33\%} = \frac{\frac{R_s}{R_0}_{measured}}{\frac{R_s}{R_0}_{33\%}} \quad , \ if \ 0\% < RH < 59\% \\ \frac{R_s}{R_0}calibrated_{85\%} = \frac{\frac{R_s}{R_0}_{measured}}{\frac{R_s}{R_0}_{85\%}} \quad , \ if \ RH \geq 59\% \end{cases} \tag{3.5}$$

For the calculation of the calibrated ammonia concentration equation (3.3) is still used, with the only difference being the use of the calibrated air fraction, instead of the originally calculated without accounting for temperature nor relative humidity.

3.2.2. BME280 sensor

The comparison experiment with temperature and relative humidity sensors allowed, amongst other things, for a comparison with a reference sensor. As such, the chosen sensor was calibrated in relation to the reference sensor. For this, the mean error between them was calculated for both variables and added to the values of temperature and relative humidity in order to approximate the BME280 readings to the correct values.

Therefore, the final values of T and RH present in the code in annexe follow the following equations (3.6):

$$\begin{cases} T_{calibrated} = T_{measured} + \overline{T_{error}} \\ RH_{calibrated} = RH_{measured} + \overline{RH_{error}} \end{cases} \tag{3.6}$$

3.3. Data Logging and Presentation Systems

Initially, the data logging was to be made by two means: locally, to an SD card, and to the cloud through wi-fi with the aid of a wi-fi module or 2G with the aid of a GSM/GPRS module. The local data logging was successfully implemented and its code, for which the work of [37], [38], [39] and [40], served as stepping-stones, can be consulted in annexe. As for the communication to the cloud, several problems arose, causing various delays in the process, which in turn difficulted the possibility to establish this way of communication of the monitored data. The Arduino Uno does not have embedded wi-fi communication and therefore, the use of a module was required. The chosen wi-fi module was the ESP8266 esp-01. This choice was made because of its small size and affordability. Unfortunately, this module was all but user-friendly, frustrating the many attempts to work with it (AT commands were not

responding as they should, tested for all available baud rates, many attempts were made trying several set procedures, like, for example, flashing the ESP8266 module). Leaving the wi-fi module, another option was explored: 2G communication through the SIM900 GPRS module. This module had the advantage of having better documentation and being able to communicate to the cloud even in most remote locations (2G network is a vast network, although it is slowly being decommissioned). This module was more expensive than the first one and had a much higher power consumption. Unfortunately, the delays caused by the ESP8266 esp-01 did not leave much time to explore this line of work and as such, the communication to the cloud feature was not achieved in due time. Some alternatives were already explored (e.g.: using a Raspberry Pi board) and are listed in Chapter 5. However, upon studying the autonomy of the system in chapter 3.6, with and without this feature, it was verified that the communication to the cloud feature would undermine the viability of the station, diminishing its autonomy dramatically, which in turn diminished the system's portability.

For ease of interpretation of the locally presented data in real-time, an RGB LED (see Figure 17) was installed to use visual cues. The LED communicates with the microcontroller through three digital pins. These visual cues consisted of the LED varying its colour with the concentration of ammonia, emitting red light for high concentrations (above 80 ppm of NH_3), green light for low concentrations (below 25 ppm of NH_3), and blue light for the values in between (from 25 to 80 ppm of NH_3). These visual cues allow most of the people to understand their situation because the colours are intrinsically associated with good (green) or bad (red) feelings, bypassing the need to understand the quantitative meaning of the presented data. For a local quantitative display of the information, the LCD displays the waiting time and the three main variables being monitored: temperature, humidity and ammonia concentration; communicating through the I_2C protocol and thus being connected to the I_2C multiplexer breakout board.

3.4. Wiring

The electric system of the QAPTs AQS started out as many prototypes do for testing: with a simple breadboard and jumpers to connect the various devices. This first form was good for experimenting when learning how to make the necessary connections but, as the circuit started to incorporate more devices, it became very intricate because of the number of jumpers used. This not only made the system very sensitive to movements in the device (the jumpers could easily be inadvertently disconnected from their places in the breadboard) but it also made it difficult to do trouble solving if any of the jumpers were unintentionally pulled. The electric circuit using the breadboard went through several stages of tests and devices used, having ended up as can be seen in Figure 19. This system included the following devices: an Arduino Uno board, an RGB LED, an MQ137 module, a BME280 sensor, a TCA9548A I2C multiplexer breakout board, a 16×2 LCD, a Tiny RTC module, a pack of eight AA batteries connected in series, an on/off switch and a micro diaphragm air pump.

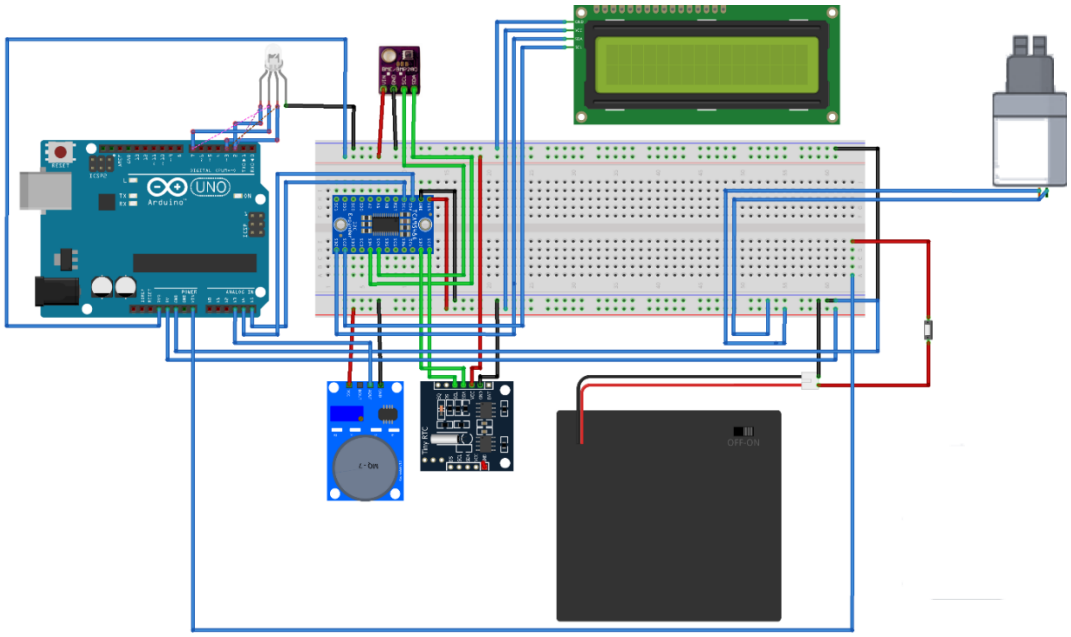

Figure 19 - Electric diagram of the QAPT using the breadboard (made in Fritzing)

In order to make the circuitry more robust, enabling the QAPT to be used in field conditions, for example, being carried or monitoring in movement, the breadboard and jumpers connections were replaced by a PCB (printed circuit board). This PCB occupied a smaller volume in the case and was designed in Fritzing, being made using a transference method with acetone from the paper to the copper sheet. The paint from the paper was transferred and protected the copper from being etched by the ferric chloride bath, leaving only the finished PCB circuit. The PCB was drilled according to the needed connections and the devices were then soldered into it. The process can be seen in Figure 20.

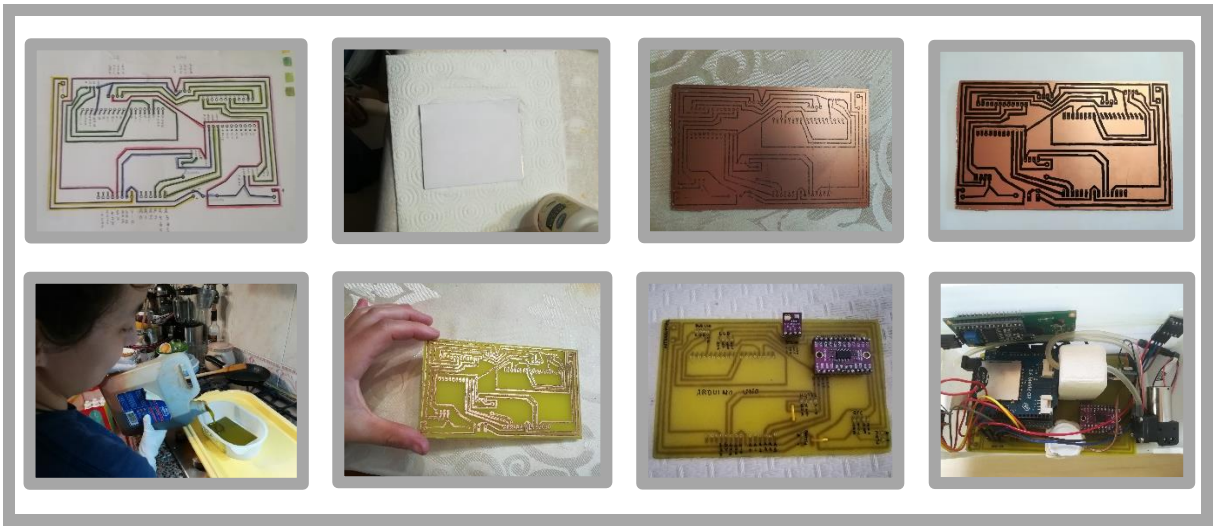

Figure 20 - PCB creation process

3.5. Prototype Case Design and Build

In order to have efficient space utilisation and meet all its specific needs, the case of the QAPT AQS was designed from scratch using SketchUp. This allowed to easily create the three-dimensional design of the case, which went through several forms that varied mainly in the type of air inlet. The two main case types were 3D printed: the case with inlet fins, that was adapted to the use of a fan, and the case with the small opening, adapted to the use of the micro diaphragm pump for the closed air sampling system (see photos in annexe C). The latter case, as seen in Figure 21, was printed in several segments in an Anet A6 3D printer (printing time of approximately 22 hours), which can be seen in Figure 22.

Figure 21 - QAPTs case with a computer for scale

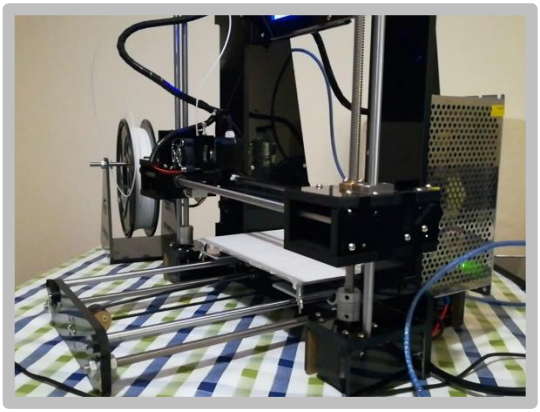

Figure 22 - Anet A6 3D printer

The printed case has a slot for the battery pack, making it easily accessible from the bottom in order to change the batteries if needed, without giving access to the interior of the station. The case is divided into two parts: the main body and lid. This lid is made so as to when removed, expose both the back and the upper side of the QAPT AQS in order to facilitate access to the interior. This makes the monitoring and exchange of sensors and other devices easier.

The case is more resistant to corrosion than normal metallic cases because it is made of a very durable plastic: PLA (Polylactic Acid). This plastic is biodegradable and can easily be recycled because it is a "thermoplastic" polyester, maintaining its properties without significant degradation when melted for other uses. This case allows the QAPT to be connected to a computer or be autonomous and has a switch that allows the user, when in autonomous mode, to turn the station on or off. As a detail, it has the name of the station inlaid in the front of the case.

3.6. Power Systems

The QAPT station was initially powered only via a USB B cable connected to a computer. This alone did not allow the system to be portable and, as such, other alternatives were studied to complement the power system. Given that the Arduino needs a power source with a voltage of approximately 9 to 12V when powered through the V_{in} pin, the first portable solution for the system was a simple 9V battery. This had the inconvenient of lasting very little time, which compromised the portability of the system, and of being a costly battery. Moving on, two other alternatives were studied: the use of a solar power bank and the use of a battery pack.

The solar power bank, as most of the power banks, had an output voltage of 5V and a maximum current of 2100mA, with the connection to the Arduino being made through the USB port. As expected, the power bank took a long time to charge with the sunlight, which could be a problem because the system consumed power faster than it recharged. As such the battery pack was also added and incorporated in the QAPT station, as a backup system with 8 rechargeable AA batteries connected in series (9,6V total voltage and 2500mAh capacity). The three possible vias to supply power to the QAPT are shown in Figure 23.

Figure 23 - 3 possible ways to supply power to the QAPT

The total current drawn by the QAPT AQS was measured with a multimeter in series, being of 270mA. With this value and with the capacity of the power bank and battery pack, the autonomy of the system was calculated: with both systems fully charged the QAPT AQS had an autonomy of approximately 28 hours of continuous monitoring.

In order to do the dimensioning of the system for future communication to the cloud, it was observed that the autonomy of the system would be much lower in this situation. This is true be it with the use of a GPRS module (consumption of approximately 2.1A) or with the use of a Raspberry Pi board ("Rasp"), as will be further discussed in chapter 5 (consumption of approximately 2.5A). The vast differences in autonomy can be seen in Table 3.1.

Table 3.1 - Autonomy of the different power systems for several communications arrangements

	Capacity	*Autonomy*	*Autonomy with GPRS*	*Autonomy with "Rasp"*
9V battery	550 mAh	2.0 h	14 min	12 min
Solar Power Bank	5000 mAh	18.5 h	2.1 h	1.8 h
Battery Pack	2600 mAh	9.6 h	1.1 h	56 min
Power Bank plus batteries	7600 mAh	28.1 h	3.2 h	2.74 h

3.7. Performance Trials

Tests to the response time, to the heating time and to the stability of the ammonia sensor were made. These led to the subsequent improvements of the code that allowed to achieve more significant results in the monitoring process, such as making an arithmetic mean of three seconds to lower the effect of the MQ137 instability in the monitored data or implementing a waiting period of 15 minutes before starting the measurements for the sensor's resistance to heat up.

In order to perform tests with the QAPT in real-life scenarios, 5 locations/trial situations were chosen: public toilets, near road traffic, horse stable yard, poultry farm, and a hair salon. These trial scenarios were chosen because they had eventually higher amounts of ammonia.

The two first scenarios (near road traffic and public toilets) were tested in one trial that combined both in a walk along a busy road ending in a public bathroom. This walk had a duration of approximately 50 minutes of monitoring.

The horse stable yard was visited on a cold and windy day. The horse's stables were located on a porch inside a farm. They were cleaned every morning and the experiment consisted of monitoring with the AQS the stables for approximately one hour in which the horse's beds were tested as well as the area around their stables.

The hair salon was studied in a period of monitorization of approximately 2 hours in which most of the time the QAPT was static, having only been displaced when a different product was used or when moving from a less ventilated room to another with better ventilation in order to study the influence on ammonia concentrations.

Finally, the poultry farm was visited on a warm day and the monitorization was carried out in a space with thousands of poults that had been in that same space for approximately four weeks. The trial was again done in motion to study the spatial distribution of the monitored data.

The data from the monitorization of the different scenarios was logged to the SD card and later studied and used in the following sub-chapter.

3.8. GIS Integration

Two of the trials, the first one and the one at the hair salon, were made with a simple addition: the use of a cellphone GPS. The phone recorded the locations and their respective timestamps during the monitorization. This data was logged to a CSV file which was later complemented with the data logged data from the QAPT. The file was then used as an input in the free GIS program QGIS. In the program, it was then possible to map the monitoring route and show the spatial distribution of the measured concentrations of ammonia.

4. Results and Discussion

This chapter covers the reference trials of the several sensors used, as well as the results of the measurements attained with the developed system. The concept of the portable system is proved through its use on performance trials to selected environments with potential ammonia-related issues, also performing GIS integration of the data collected.

4.1. Characterisation and Reference Trials

4.1.1. Ammonia Sensor

As the ammonia sensor used is a metal-oxide semiconductor, it needs to heat a resistance in order to be able to monitor more selectively the concentration of ammonia. As such, the heating time of this resistance was considered to be of 15 minutes: that was the minimum time interval in which the measured concentration was observed to stabilize to values below the range of detection of the sensor (below 5 ppm of ammonia). The heating time waiting period, conducted before the beginning of the monitorization periods, led to more consistent responses of the sensor when exposed to the targeted gas.

The sensors responses were induced by exposing the surrounding air near the air inlet to a liquid ammonia sample, that quickly evaporated when uncovered, and thus triggering the response of the sensor. In one of these trials, the exposure was so high that the sensor became unreactive, which indicated that it had saturated. To solve this issue, the sensor was left working in an ammonia-free environment for approximately three days. This procedure restored the sensor sensibility to its normal capacity and exposed its limits. Although it is very unlikely that the sensor will be exposed to such concentrations when monitoring outdoor or indoor air quality, this occurrence is still a reminder of the limits of the equipment and its potential usages.

With the initial data logging being done with a set interval of 1 second, it was verified that there were fluctuations in the response of the MQ137 sensor that did not correlate with observed changes in ammonia concentration. Therefore, with the application of an arithmetic moving average of the values acquired in three seconds, the “noise” that was seen as the fluctuations in the measurements was significantly reduced, improving the data representativeness.

Also, it was verified that the calibration with temperature and relative humidity improved the correlation of the measurements to the real concentration of ammonia, significantly diminishing the variation of the measured concentration with the influence of temperature and relative humidity, as was intended.

Unfortunately, with the lack of a reference ammonia sensor, it was impossible to calibrate the MQ137 sensor with reference to it. As such, the ammonia concentration that this sensor measures might not be the most accurate, as the values were not corrected with data from a reference sensor. However, the measured concentrations and their variations are within the expected value ranges, as will be further shown in Chapter 4.6.

4.1.2. Temperature and Relative Humidity Sensors

The data logged from the comparison experiment between the three types of temperature and relative humidity sensors was plotted against the measured values of the reference sensor (Telaire), as can be seen in Figure 24 and Figure 25. These figures show the reference sensor's values, in black, following the $y = x$ equation. Ideally, all the sensors readings should be as close as possible to the reference sensor, and as such, as close as possible to the $y = x$ equation.

To perform the reference trials of the temperature and relative humidity sensors, six sensors were tested, as depicted in Figure 24. It is observable, by the horizontal lines of points in dark orange and light blue, that both DHT11 sensors are less sensitive to changes in relative humidity than the remaining sensors, changing their output values in larger intervals than the others. Another patent observation is that both BME280 sensors (dark blue and green) have systematically lower values than the reference sensor; oppositely, the DHT22 sensors have systematically higher values than the reference sensor. This difference is of approximately the same amplitude for all of the sensors in the DHT11_1, meaning that the module of the distance to the reference line is similar.

It is also clear that the DHT22 sensors have a slightly higher dispersion than the BME280 sensors (spatial dispersion of the data) and that both the sensors datasets of each family have slightly different slopes, indicating that this is an individual characteristic of each sensor and not just a factory set.

From this figure, it was then possible to select the two most interesting sensors, which were closest to the reference line, with less dispersion and with a similar slope to the reference: the DHT22_2 (in grey) and the BME280_2 (in green).

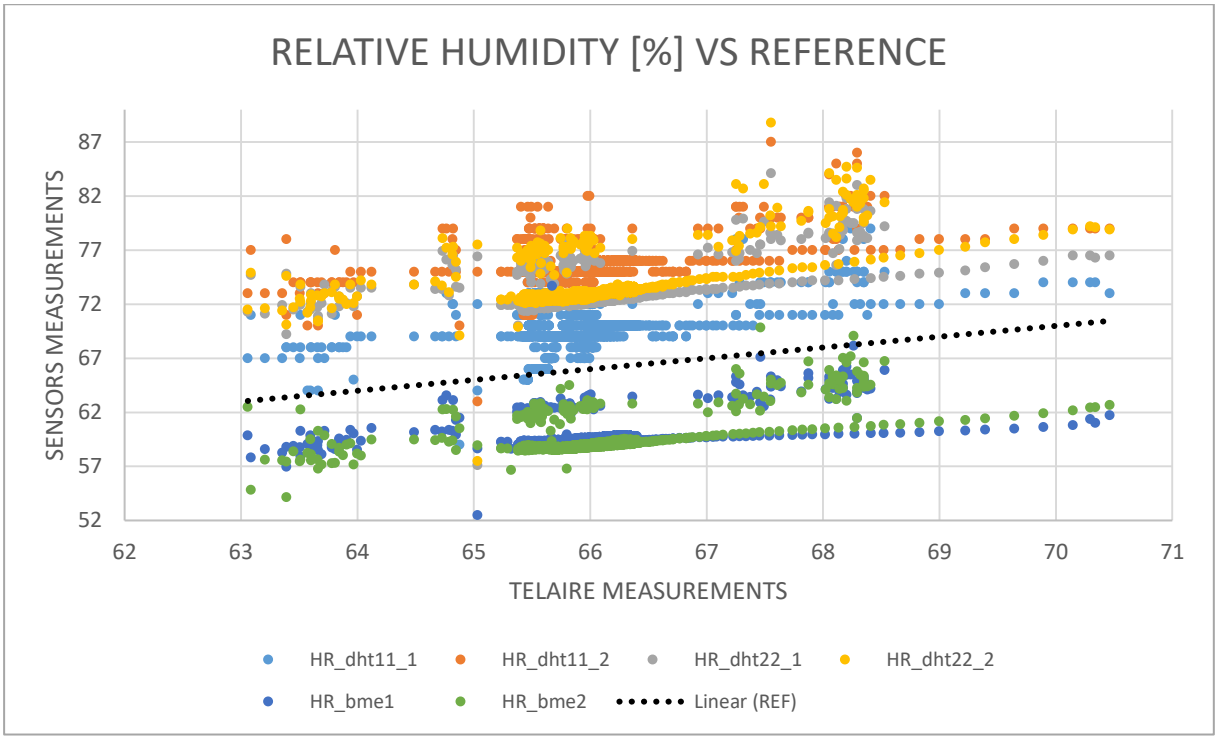

Figure 24 - RH experiment results: sensors vs reference (Telaire)

Regarding the temperature reference trials, Figure 25 depicts a very different situation. In this figure, all of the sensors present lower values when compared to the reference sensor and the sensors which have the closest values are the sensors from the BME280 family. Contrariwise, the sensors that present the farthest values are both the dht_11 and the DHT22_1. It is also possible to note that all of the sensors change their behaviour from the interval between 20.5℃ and 21.2℃ on. In this interval, the BME sensors are even closer to the reference than in the remaining temperatures, which is especially interesting given that the mean temperatures in closed interiors are usually between 18℃ and 22℃ and that the mean temperature in Portugal is below the 21.5℃ limit, value that marks the increased (but constant) error between the BME280 sensors and the reference sensor.

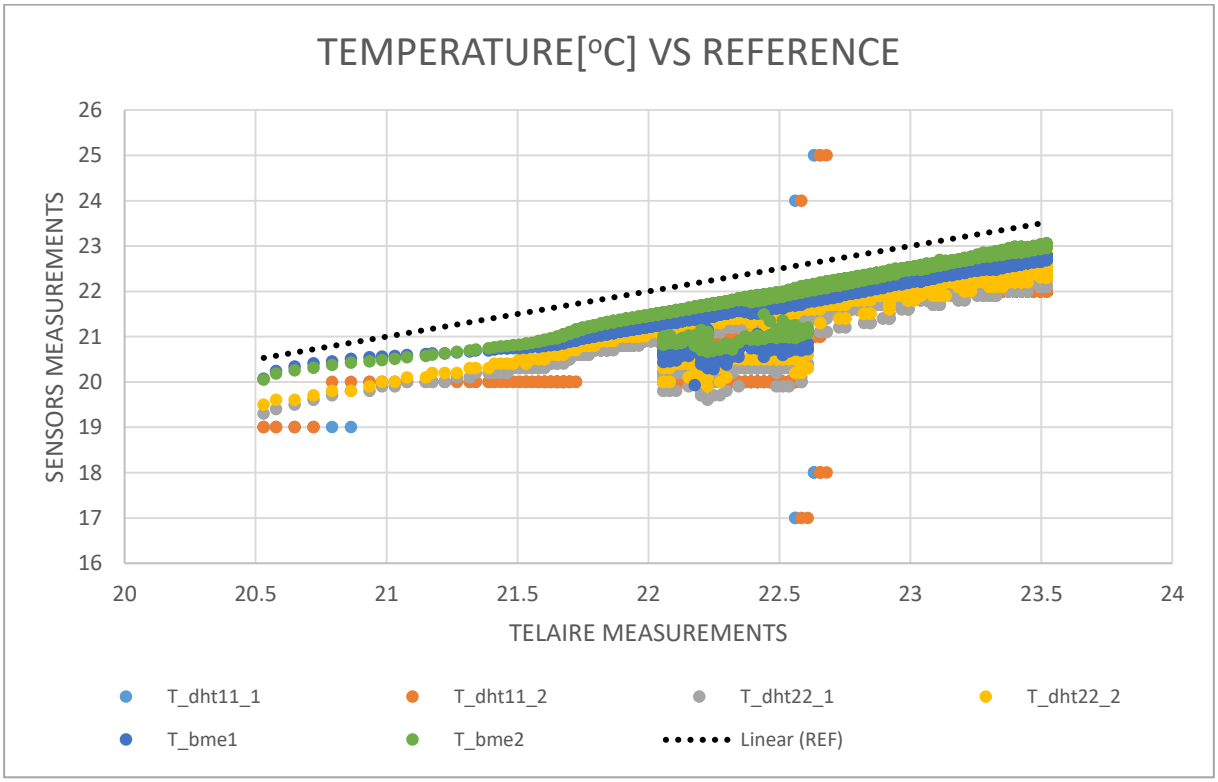

Figure 25 - T experiment results: sensors vs reference (Telaire)

The absolute variation around a determined value shows the distance of the analysed data in relation to the said value. In this situation $(x - \bar{x})$ this value will be both the mean temperature and the mean relative humidity. With the depiction of these variations versus one another, as can be seen in Figure 26, one can easily evaluate the dispersion of each sensor's acquired data in relation to its mean values and to the other sensors. Once again, with the Telaire sensor as reference, the clouds of points should be as close as possible to the black dots, and be as small as possible. For better visualisation of the data, this graphic was separated into three figures, Figure 27, Figure 28 and Figure 29, depicting the three different sensors families, DHT11, DHT22 and BME280, respectively.

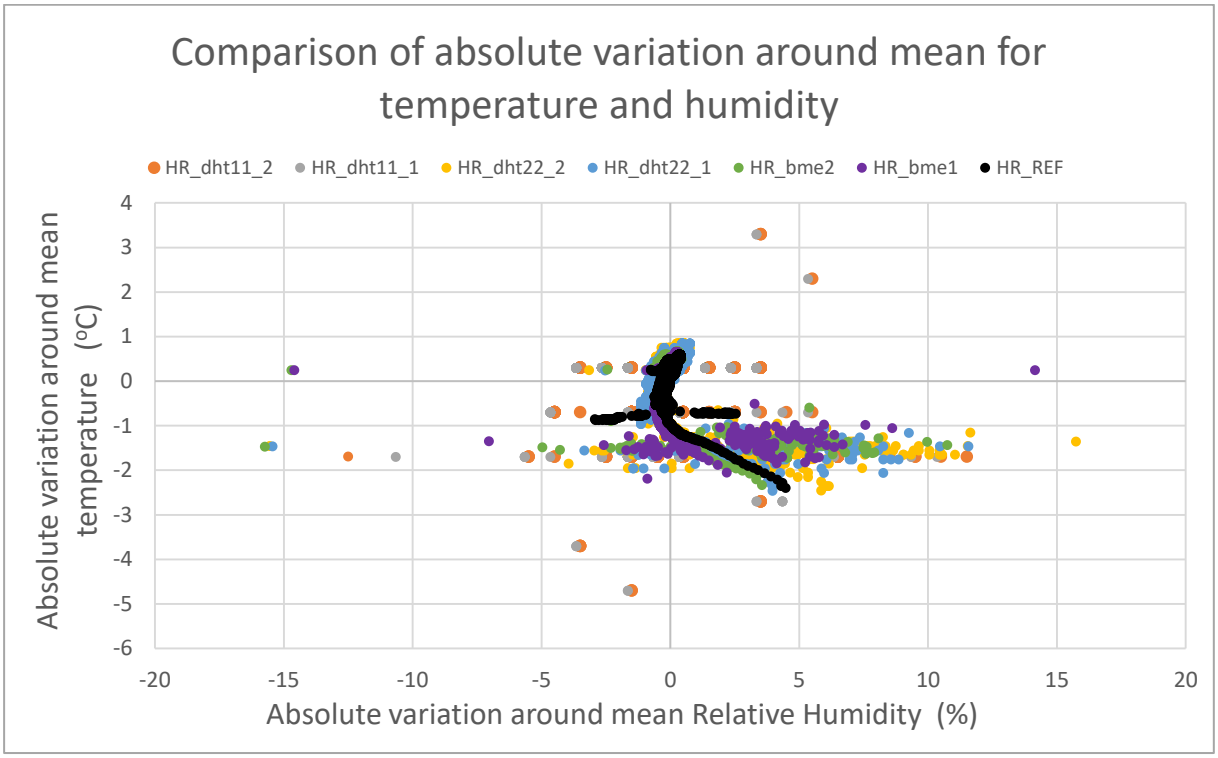

Figure 26 - Absolute variation around Tmean vs abs variation around HR mean

In Figure 26 we can see that the DHT11 sensors, depicted in dark orange and grey, have the most accentuated dispersion in temperature when compared to the other sensors. Another very visible aspect is that **all** the sensors have a much higher dispersion in the relative humidity data than in the temperature data.

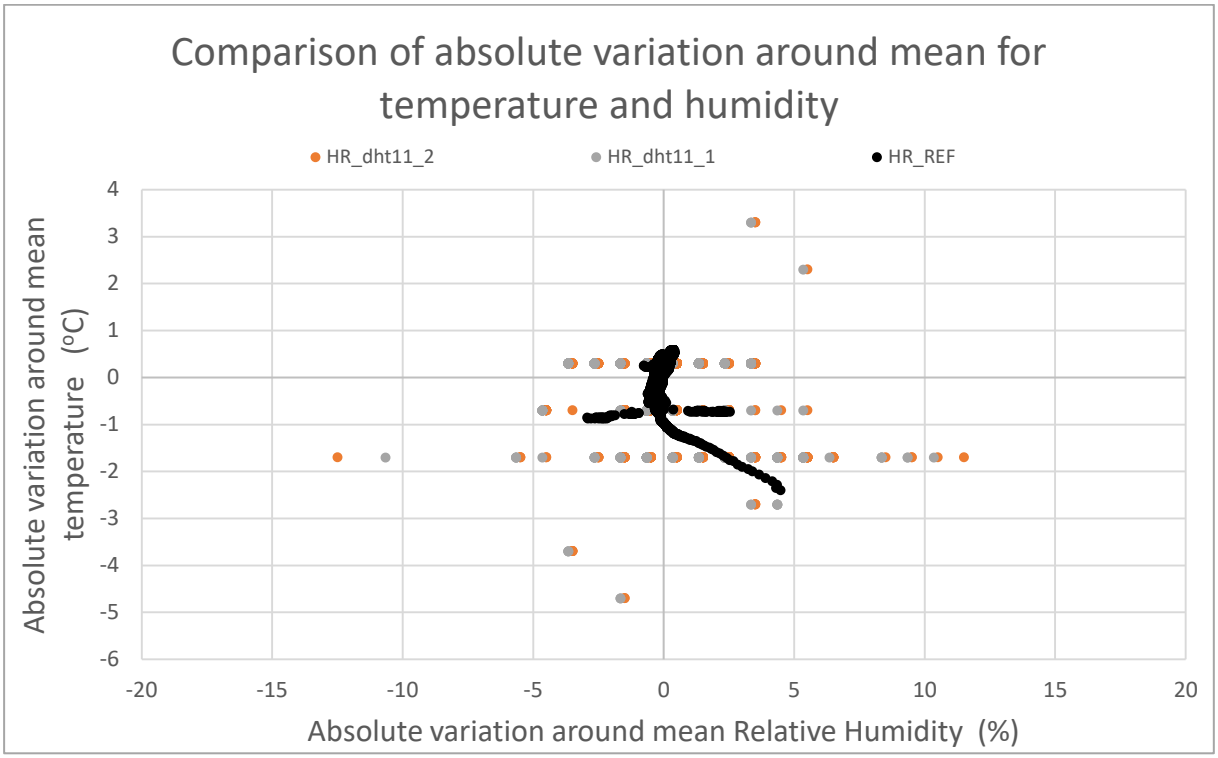

Figure 27 - DHT11 sensors family - Abs variation around Tmean vs abs variation around HR mean

Focusing on the DHT11 family sensors depicted in Figure 27, one can observe that both their variation in temperature and in relative humidity are very accentuated, being easily understood that these sensors have much bigger steps in the measurements, demonstrated by the space between the lines of points, than the reference sensor. This happens because their output has a unitary resolution. It is also apparent that the dispersion is much higher in relation to the relative humidity measurements than to the temperature measurements, which is corroborated by the sensor's datasheet [41]: accuracy of ∓5% for relative humidity and ∓2℃ for temperature. Both DHT11 sensors present the same behaviour.

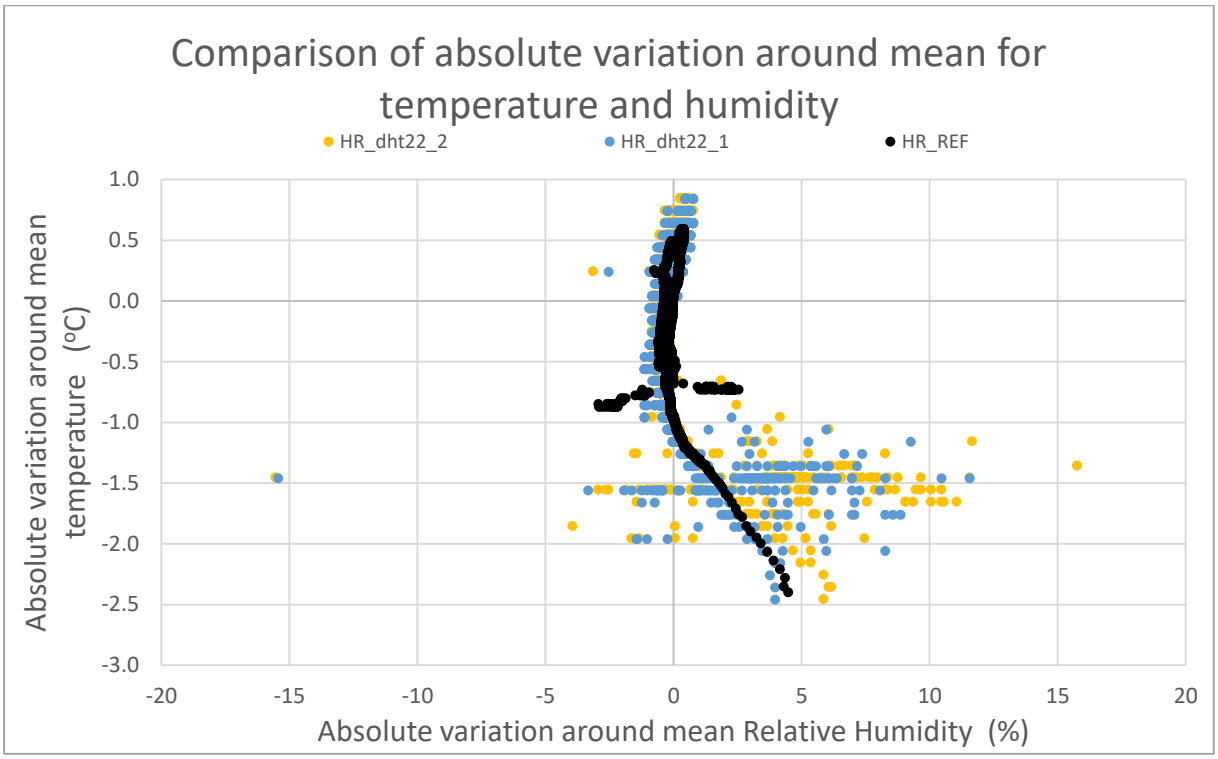

Figure 28 - DHT22 sensors family - Abs variation around Tmean vs abs variation around HR mean

In this figure (Figure 28), it is possible to observe that the clouds of points from the DHT22 sensors are much closer to the reference when compared to Figure 27. It is patent that there are still reading steps in the measurements, but these are much smaller than those from the DHT11 sensors. This behaviour was expected since the DHT22 sensors have a higher resolution than the DHT11 [42]: 0.1% for relative humidity measurements and 0.1℃ for temperature measurements. In terms of accuracy, it is also possible to see that the DHT22 sensors have a much higher accuracy, being, therefore, closer to the reference measurements: accuracy of ∓2% for relative humidity and ∓0.5℃ for temperature [42]. Lastly, it is also observable that there is a cloud of points, with more dispersion than in the remaining plot, that is related to the measurements seen in the reference measurements as a horizontal set of points. This cloud is a good indicator of the real accuracy of the sensors and by comparing the centre of each data set (the clouds from the DHT22 sensors to the reference sensor) it was possible to see that the DHT22 sensors were measuring with an absolute variance of $-0.9℃$ and $+5\%RH$, which surpases the accuracy from the datasheet in both parameters, to both DHT22 sensors.

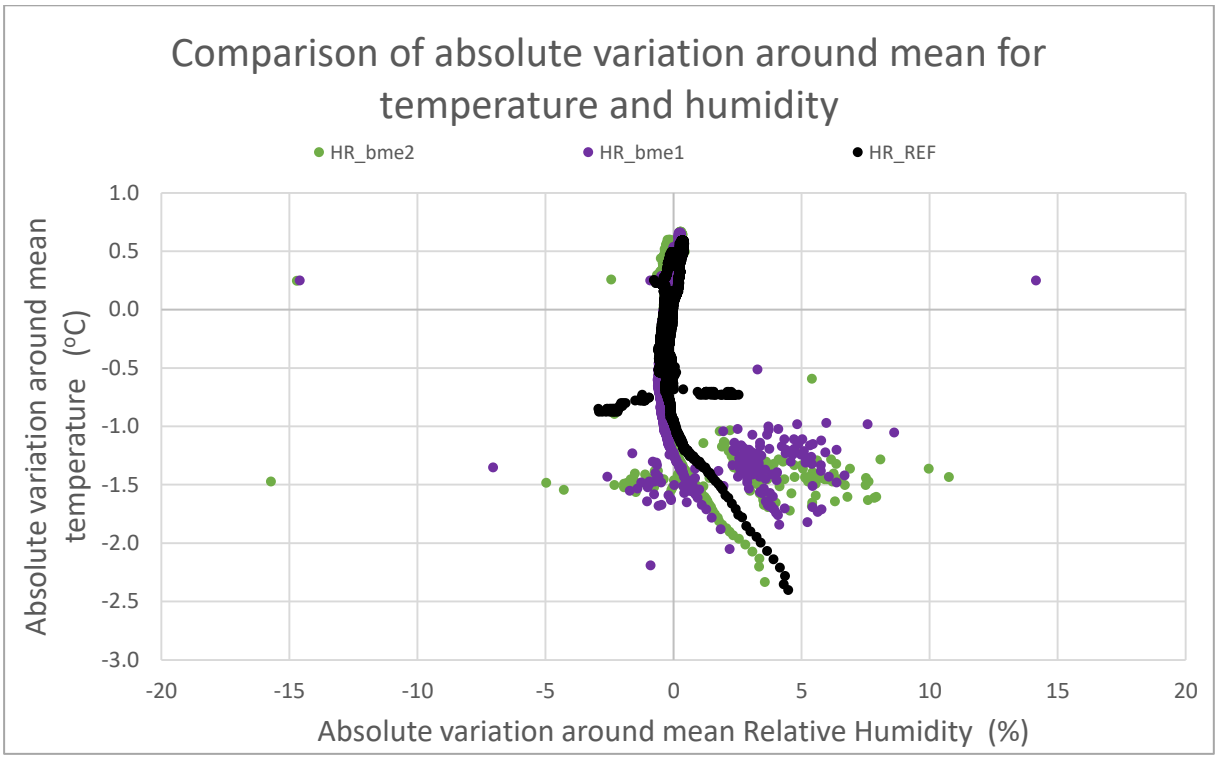

Figure 29 - BME280 sensors family - Abs variation around Tmean vs abs variation around HR mean

Lastly, but not least importantly, in Figure 29, one can see the behaviour of the BME280 sensors. These present the smallest dispersion in relation to the reference sensor in both relative humidity and temperature measurements, with no visible steps in the depiction of the data. This was expected due to their higher resolution [43]: 0.008% for relative humidity measurements and 0.01℃ for temperature measurements.

Such as in Figure 28, it is also observable that there is a cloud of points, with more dispersion than in the remaining plot, that is related to the measurements seen in the reference measurements as a horizontal set of points. However, this cloud of points has a lower dispersion than the latter, which is a result of BME280 sensors accuracy: accuracy of ∓3% for relative humidity and ∓0.5℃ for temperature [43]. Comparing the centre of the reference points and the cloud it is then possible to observe that the BME280 sensors are consistent with these values: of +2.5% for relative humidity and −0.7℃ for temperature; also closer to the reference sensor than both the DHT sensors families.

As such, the sensor chosen to be incorporated in the QAPT AQS was from the BME280 family, particularly the BME280_2 sensor. This sensor was then calibrated in relation to the reference sensor, by calculating its mean error for temperature and relative humidity and making the corresponding adjustments, as can be seen in equation (3.6), with both the temperature error and the relative humidity error (0.55℃ and 6.89%, respectively).

4.2. Memory usage and stability

During the experiment presented in sub-chapter 3.1.3, some stability problems were encountered, particularly with the data logging of the measurements. These were the first signs that the Arduino Uno might not be the most appropriate development board for the QAPT.

These instabilities, derived from the complexity of the code, were largely solved with the improvement of the code's performance in terms of memory usage (Arduino sketch used 73% of the dynamic memory and 68% of the memory storage). Still, some sporadic lapses occurred in the data logging and RTC functioning, which led to the need for an interpolation of the data.

In order to solve this problem, there was a compromise between the amount of data logged variables and their registered resolution. With only the most important data being data logged (date, time, relative humidity, temperature, height and ammonia concentration), there were still some lapses and as such the values had to be treated as *ints* in order to completely solve this problem. This action did not affect the sensor's calibration (because the calibrations were made with the measured variables being treated as *floats*, and as such with no loss of information in the calibration process) nor, subsequently the ammonia concentrations measured (as the MQ137 sensor did not have a higher resolution than unitary).

With this compromise, the QAPT AQS did not have any further issues of systems' stability. Still, if more sensors were to be added to the system, these problems might arise again, with the increase in the code's complexity and size. Therefore, the use of the Arduino Uno board might not be the best solution in future works and other alternatives might be of interest, as will be further discussed in chapter 5.

4.3. Air Sampling System

The two tested air sampling systems varied in two main things: the device used for the air admission and the sharing or not of common space with the electrical systems.

The first air sampling system used a $5V$ fan to impose the air extraction and shared the common space of the full interior of the QAPT's case. This system faced several problems: the thermal load of the electrical system directly influenced the air samples being analyzed and as such, not only did the temperature rise but the relative humidity would also lower during the length of the experiment; the other problem was no less critical because the system was experiencing a significant lag (of more than two minutes) in the sensors response time (measured by exposing the neighbouring environment of the QAPT to a liquid ammonia sample, which would quickly evaporate and should create positive detection by the MQ137 in very short exposure times).

Besides, even after detection by the MQ137 sensor, its values were sometimes much lower than the expected with the exposure to such high concentrations of ammonia. One last problem might happen with this arrangement: the ammonia might have adverse effects when in direct contact with the circuitry of the AQS. Although ammonia gas is not considered a flammable gas by definition, it should be treated as one for safety and has a lower explosive limit of 15% per volume of air [44]. This limit might seem high and safe enough, but with circuitry increasing the interior air temperature (that lowers the lower explosive limit) and with the eventually high exposure to ammonia the AQS could be subjected to this direct contact might become an imminent danger. This high exposure could also corrode the system's

devices and circuitry, damaging it and leading to the QAPT's deterioration with use (and consequent exposure).

The second and final system being studied consisted of a closed air sampling system that used a micro diaphragm pump for air extraction. Separating the air sampling system from the electric system solved most of the difficulties encountered in the first studied system. The thermal load of the electrical system no longer influenced the sensors (BME280 and MQ137) because they were only being exposed to the outside air. With this solution, the thermal load's effect greatly diminished, and the only thing that could influence the temperature and humidity sensor measurements was the MQ137 thermal load. To solve this issue, the sampled air was made to go through the BME280 sensor first (to measure the outside air temperature and humidity) and only then through the MQ137.

With the extraction being done in a closed circuit, the sampled air was measured in a much faster way because the air renovations were much faster. This solved the problems with the amplitude of response and lag of the system and as such the response time of the QAPT was only limited by the response time of the ammonia sensor itself (maximum of 30 seconds).

This system solved one other problem: the target gas does not come in direct contact with the electronics. As such, the flammability danger and the corrosion of the system are greatly diminished, fact that increases the lifetime of the system and diminishes eventual maintenance costs. Besides, the diaphragm pump does not need any kind of lubrication oil that might interfere with the composition of the sampled air and as such, this pump is especially interesting for the use in air quality monitorization, keeping the sampled air unchanged.

One other interesting feature of the installed diaphragm pump is that it allows the airflow control with a variation in the voltage. This might prove interesting for further studies in order to maintain the isokinetism of air sampling.

Ultimately, this air sampling system allows the sensors to be inside the QAPT's case and not outside where the airspeed of moving measurements might affect its results.

4.4. Wiring and Power Systems

The electric system of the QAPTs air quality station had its stability greatly improved with the use of the printed circuit board, without further need for adjusting jumpers with poor connections and increasing the available space inside the case.

The stability of the system was very important in order to be able to do the monitorization of air quality in movement and transport the station without inflicting damage to any of the devices or electric connections. This improvement was only possible/viable when the electrical scheme stabilized, with no intentions of further changes in layout, because the PCB was made as a final circuit, without space for large alterations in order to occupy the smallest possible space.

Having more space inside the case, it can be easier to install more air quality sensors, magnifying the possibility to make the QAPT a more complete air quality station in further studies. For the users, this extra space is also helpful as it allows for more ease in the maintenance of the different devices in the interior.

By doing several trials with the QAPT, it was observed that the electric system had different thermal loads depending on the type of power system used. Both with the computer as the power source and with the power bank, the temperature and humidity inside the case maintained their values practically unchanged in relation to the outside air temperature and humidity. On the other side, when the battery pack was used to power up the system, the temperature gradually increased inside the case ($0 < \Delta\overline{T} <$ 4℃) and the relative humidity decreased ($0 < \Delta\overline{RH} < 10\%$). This variation stressed the advantage of the separation of the air sampling system from the electric system, which allowed the MQ137 and BME280 sensors to keep measuring the outer temperature and relative humidity without being significantly affected by this phenomenon.

Investigating further the distribution of heat inside the case with the use of a thermographic camera (FLIR E6) it was verified that the heat was mainly coming from very specific parts of the system: the MQ137 sensor and the Arduino's voltage regulator, as can be seen in figures 30 and 31, and further observed in annexe D. This led to the conclusion that the voltage regulator was dissipating much more heat when the system was connected to the battery pack (see Figure 30) because it needed to adjust the approximately $10V$ input to the $5V$ and $3.3V$ output used in the circuitry. It also explains why there was no significant increase in temperature when connected to the other two power sources (see Figure 31) as both had an input of $5V$ regulated through the USB which put the voltage regulator under much less stress.

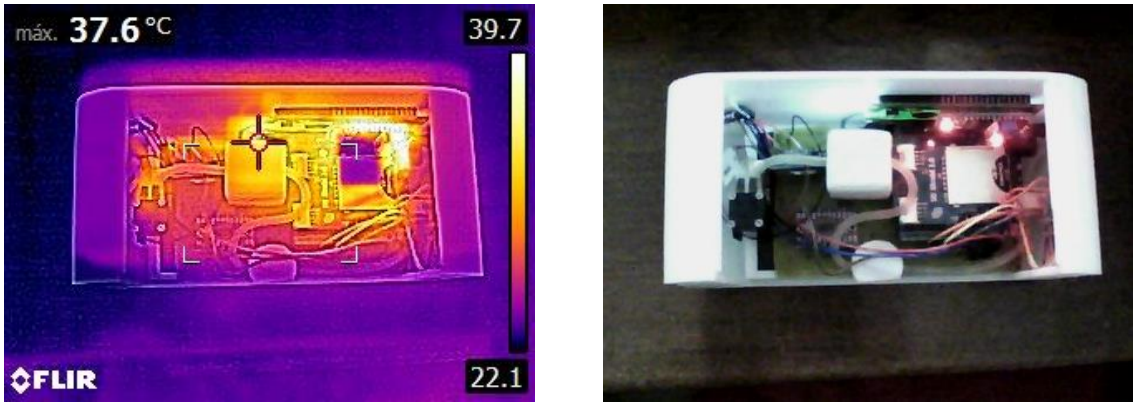

Figure 30 - Thermography QAPT interior powered by battery pack

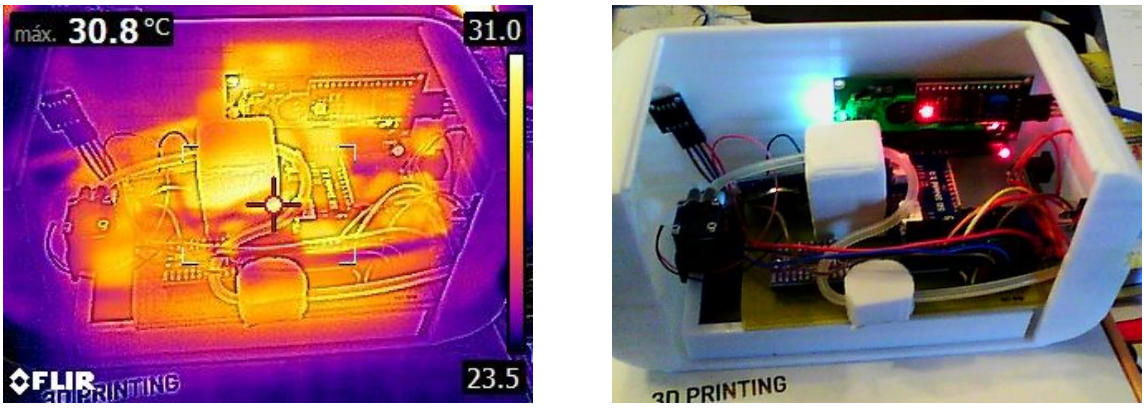

Figure 31 - Thermography QAPT interior powered by power bank

4.5. Cost Analysis

In this sub-section, the cost of the QAPT air quality station and of its elements will be discussed as well as the cost of the two other alternatives for the QAPT with access to the cloud: one using a Raspberry Pi 3 board (Alternative 1) and the other using a GPRS/GSM SIM900 module and Arduino Uno board (Alternative 2). Both these alternatives were conceptually studied but did not proceed to the test stage due to a lack of time to do so.

4.5.1. QAPT System

The QAPT's components costs can be found in Table 4.1, ordered from the least to the most expensive. In this table, it can be seen that the **total cost of the QAPT is of roughly 133€,** which is **well below the 200€ threshold**, as was initially pretended, making this a portable and effectively **very low-cost air quality station**. It is possible to note that the second most costly component of the system is, in fact, one, if not, the most important: the MQ137 ammonia sensor.

As can be seen in Figure 32, the most costly sector of the QAPT is, as expected, the air sampling system, that includes both the sensors and diaphragm pump, weighing 43% of the total cost of the air quality station. The next most expensive sector is the power system (vastly because of the power bank and rechargeable batteries), being closely followed by the electronics components that encompass, among others, the Arduino board. The least expensive sector is the user interface sector, weighing only 2% of the total cost of the air quality station, which corresponds to less than 3€. The low cost of this sector comes as a good surprise because this sector, although not essential to the functioning of the station, enables the information to be readily comprehended by the system's users: a noble function for a modest price.

The data logging sector, comprising both the RTC and the SD card shield, accounts for 9% of the cost of the QAPT. This is one of the lowest values for the alternatives being presented in the following sub-chapters because it does not do the data logging to the cloud, that has inherent costs. The 3D printed case, cames as the second most inexpensive sector, costing only 6€, which is quite a low cost given that it was built specifically for the use in the QAPT air quality station.

The represented costs are the real cost at the moment of the purchase of the components. It is therefore worth noting that some of the components might have a higher or lower market cost depending on the date of consultation of the market (example: the MQ137 sensor cost 25€ when it was purchased, see Table 4.1, but upon later research, some were found online for even lower prices). This factor might affect the final cost of the prototypes significantly, but as the tendency of the market is usually of lowering the prices of the items, this tendency is, in fact, advantageous to this work, because the cost of this system will tend to lower with time.

Table 4.1 - Discriminated costs of the QAPT AQS

QAPT DEVICES	*PRICE [€]*
On/Off switch	0.12
LCD	1.15
RGB LED	1.55
USB A-B cable	1.73
RTC	1.95
BME280 sensor	2.23
PCB plate	3.08
I2C Multiplexer	4.32
Arduino Uno R3	4.47
PLA for 3D print	6.00
Jumper cables pack	6.85
SD card shield	10.34
Solar Powerbank	15.00
Batteries+battery pack	19.15
MQ137 sensor	25.00
Diaphragm pump	30.00
TOTAL	132.94

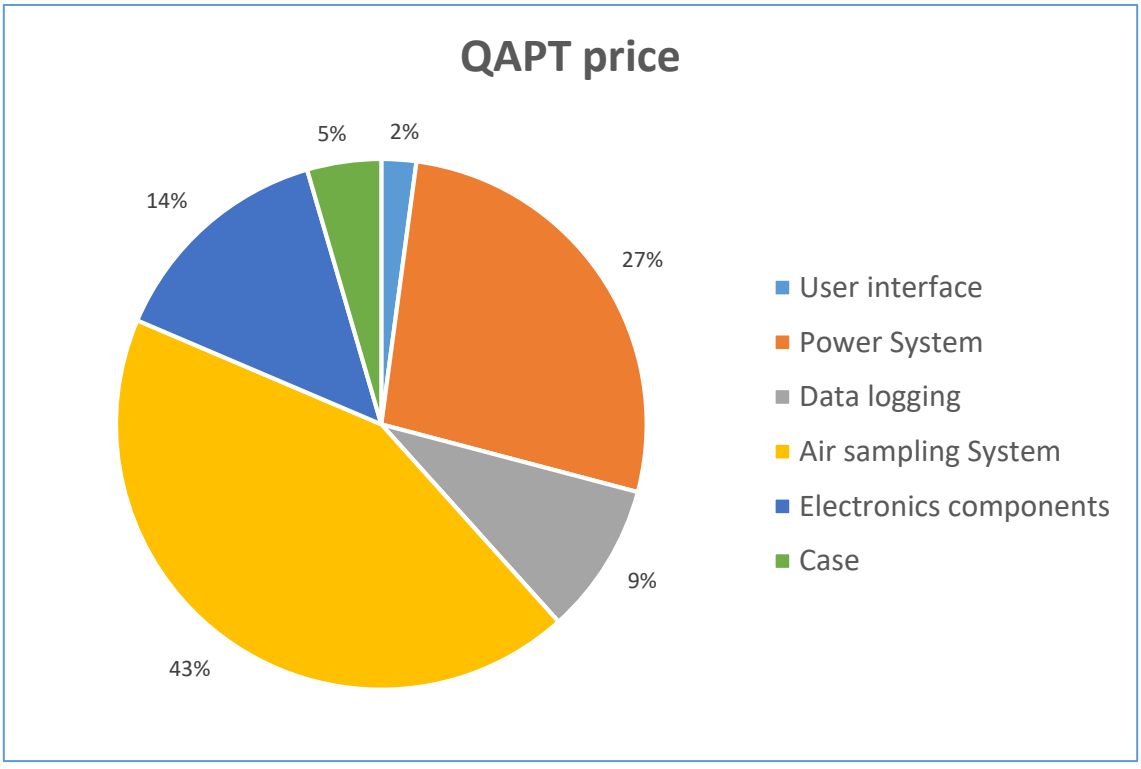

Figure 32 - QAPT components's cost distribution by section

4.5.2. QAPT System with Wifi – Alternative 1

Regarding **alternative 1**, proposed as a possible further improvement to the QAPT air quality station, the costs of each component are depicted in Table 4.2. In this table, it is possible to see that the MQ137 sensor is now the third most expensive equipment of the station. The most costly is the Raspberry Pi board, that costs roughly 37€, closely followed by the diaphragm pump. This value, that might seem high when compared with the Arduino board acquired for the station, is not so markedly high when its full capabilities are considered, allowing for easy communication to the cloud without the need for the acquisition of further pieces of equipment.

As can be seen in Figure 33, the most costly sector continues to be the air sampling system, but this time, being followed by the electronics components sector, because of the higher cost of the Raspberry Pi board when compared to the Arduino board. This sector's relative cost (27%) could also be distributed to the data logging relative cost but was allocated in its totality to the electronics components sector for ease of understanding and for its central importance in that sector.

With the increase of the systems total cost, the sectors that maintained their costs, like the user interface sector or the case, inherently acquire a smaller relative cost.

This alternative will have a higher cost due to its more **extended range of capabilities** (communication to the cloud via wi-fi, Bluetooth, increased memory space, etc.), **costing approximately 165€,** still well below the threshold considered before, and therefore a very low-cost solution.

Table 4.2 - Discriminated costs of the QAPT's Alternative 1

QAPT wifi alternative Raspberry	*PRICE [€]*
On/Off switch	0.12
LCD	1.15
RGB LED	1.55
USB A-B cable	1.73
RTC	1.95
BME280 sensor	2.23
PCB plate	3.08
I2C Multiplexer	4.32
PLA for 3D print	6.00
Jumper cables pack	6.85
SD card shield	10.34
Solar Powerbank	15.00
Batteries+battery pack	19.15
MQ137 sensor	25.00
Diaphragm pump	30.00
Raspberry Pi 3b	36.95
TOTAL	165.42

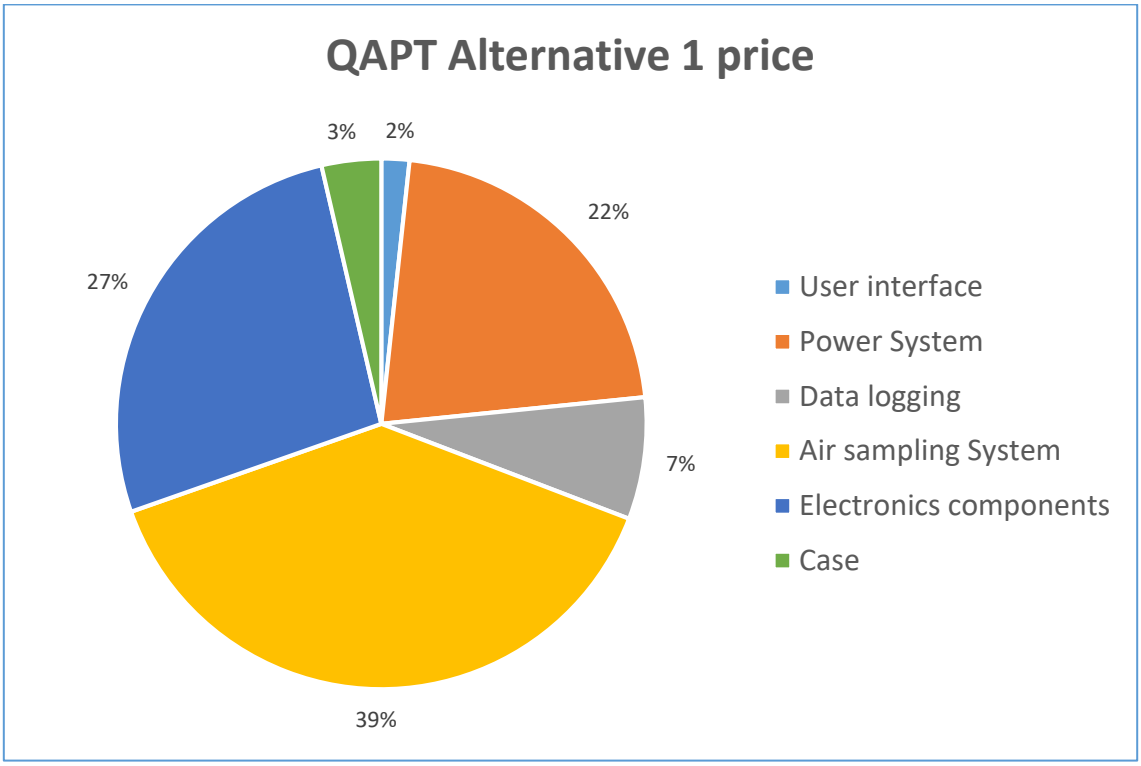

Figure 33 - QAPT's Alternative 1 component's cost distribution by section

4.5.3. QAPT System with Wifi – Alternative 2

Lastly, for alternative 2, which is presented as another way for a possible future improvement of the QAPT, the costs are shown individually for the several components, in Table 4.3. In this scenario, the MQ137 sensor comes as the third most costly component of the air quality station. Exclusive to this scenario, the utilisation of the SIM900 module comes with a significant added cost of approximately 56€, the most costly investment. This module, being responsible for the data logging to the cloud, greatly increases the relative cost of the data logging sector, as can be seen in Figure 34, with a weight of 22%, the highest of the three studied scenarios. As in the other scenarios, the air sampling system is still the most costly, with the case and user interface maintaining the values from the alternative 1.

As can be seen in Table 4.3, the total cost of this alternative is of approximately 189€. This is the most costly alternative and comes with less potential capabilities than alternative 1 (ex: no Bluetooth nor added memory space). On the other side, the communication to the cloud can be made through 2G, allowing the data logging to be made even in more isolated areas, which would be more difficult with alternative 1. This alternative also occupies a larger volume than the other two.

Table 4.3 - Discriminated costs of the QAPT's Alternative 2

QAPT wifi alternative SIM900	*PRICE [€]*
On/Off switch	0.12
LCD	1.15
RGB LED	1.55
USB A-B cable	1.73
RTC	1.95
BME280 sensor	2.23
PCB plate	3.08
I2C Multiplexer	4.32
Arduino Uno R3	4.47
PLA for 3D print	6.00
Jumper cables pack	6.85
SD card shield	10.34
Solar Powerbank	15.00
Batteries+battery pack	19.15
MQ137 sensor	25.00
Diaphragm pump	30.00
Sim900 +USB to TTL	56.30
TOTAL	189.24

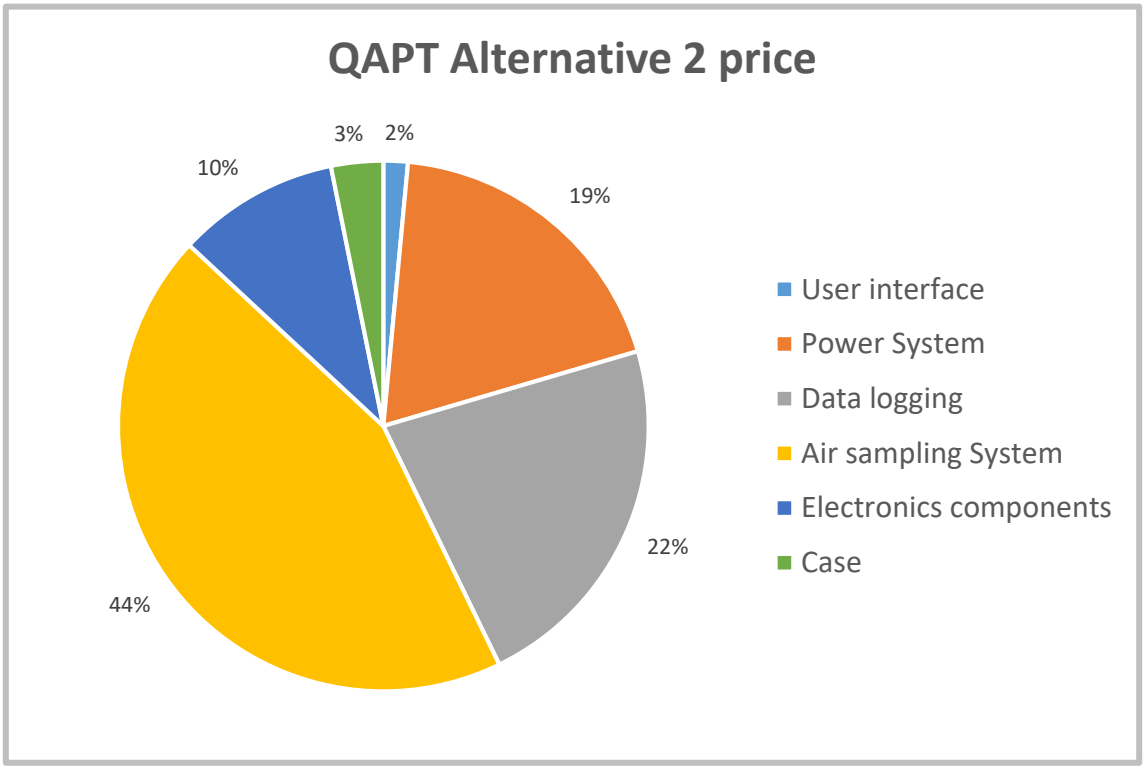

Figure 34 - QAPT's Alternative 2 component's cost distribution by section

4.6. Performance Trials and GIS Integration

In this sub-section, the results of the performance trials will be presented and discussed, as well as the results and interest of the integration with GIS software.

4.6.1. Near Road Traffic and Public Toilets

In this first performance trial, the acquisition of data was conducted following a walk along a busy street and ending in a villa, particularly in available public toilets. The concentrations of ammonia along the experiment varied very little, almost always below the measuring range, as can be seen in green in Figure 35. In the first section of the experiment, in a downhill part of the track, a car went past the monitoring area, going up the road and leaving a foul smell. A few seconds later, the QAPT AQS detected higher amounts of ammonia in the air, reaching 7 *ppm* of ammonia, as can be seen in red in Figure 35. This reaction might have been induced by a poor condition of the car engine's combustion, leaving ammonia traces, other nitrogen compounds or other gases that affect the selectivity of the MQ137 sensor, like, for example, and very likely, carbon monoxide.

The public toilets reached at the end of the monitorization, as can be seen in a bigger cloud of green dots at the top of Figure 35, were rather clean and therefore, as expected, the concentrations of ammonia were not high enough for the MQ137 sensor to detect.

The visualisation of the acquired data with the QGIS software allowed for a better spatial perception of the events, which in this case was important and served as a better means of representation than, for example, a graphic or table.

Figure 35 - Performance trial 1: car traffic and public toilets GIS track

4.6.2. Horse Stable Yard

In the second performance trial, the monitorization of the air quality was conducted in a private horse stable yard, on a windy and cold day. The horse's manure was cleaned every morning and the horse's stables were in an open yard. As such, the QAPT did not detect the presence of ammonia in this scenario because with only three horses and with their beds recently clean the ammonia must have evaporated quickly and dispersed from the monitored area.

One interesting event happened when monitoring the air quality around the stables: a horse caretaker was impregnating the guard dogs with a mixture of alcohol, cloves and coconut oil. As he was spraying them with this mixture in order to keep the flees away, the QAPT AQS supposedly detected high amounts of ammonia (reaching almost 35 ppm as can be seen in Figure 36), which were not really present in the sprayed solution. This demonstrated the limitation of the MQ137 sensor selectivity once again, as it detected the alcohol in the mixture, leading to a false positive in ammonia concentration.

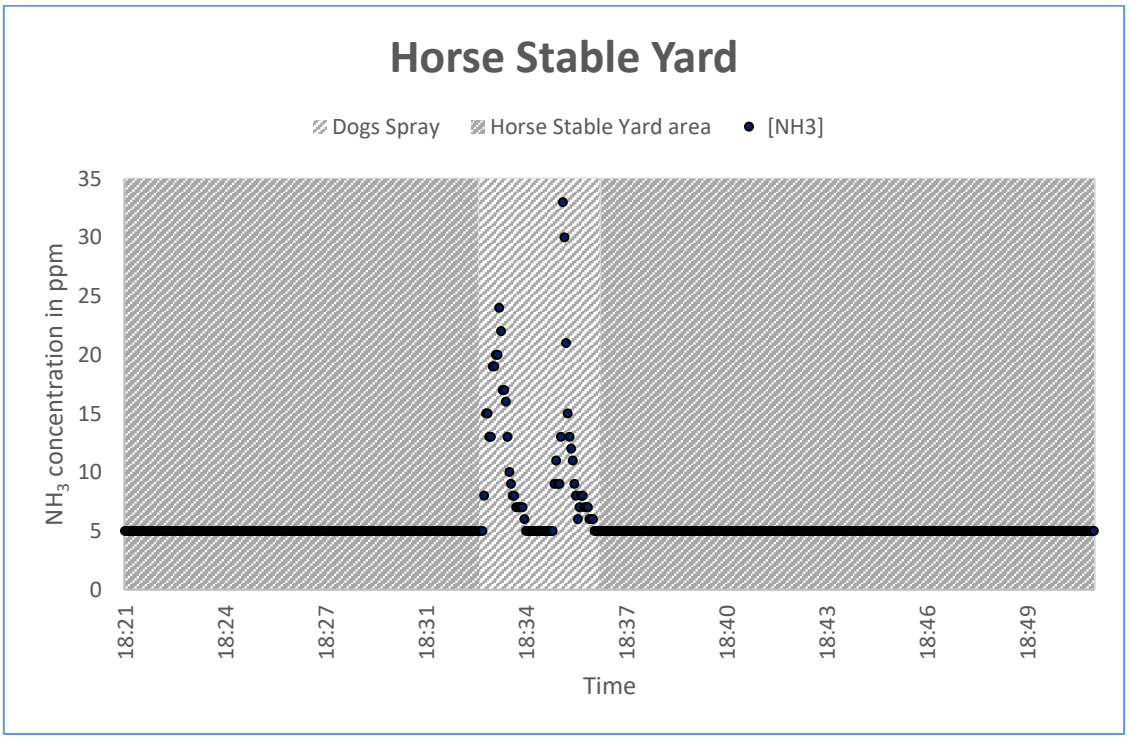

Figure 36 - Performance trial 2: horse stable yard

4.6.3. Hair Salon

In this third performance trial, the monitorization of the air quality was conducted in two ways: a moving monitorization and a quasi-static monitorization. The first, conducted by measuring the air quality along the track seen in Figure 37, was performed by placing the QAPT outside a car window and moving at a mean velocity of approximately $50\ km/h$. In this part of the experiment, no variations were measured in the range of action of the MQ137 sensor until reaching the hair salon (blue and purple dots represent 3 and 4 ppm of ammonia respectively, outside the range of the sensor and the red dot represents the measurements of the second phase of the experiment).

Figure 37 - GIS integration: monitoring ammonia in route and hair salon

The second phase of the experiment, depicted in Figure 38, started upon the arrival at the hair salon. The first noticeable thing is the immediate difference in ammonia concentration once the QAPT passes the hair salon entrance, reaching concentrations of around $16\ ppm$. Once in the hair salon, the QAPT continued its monitorization in a small area were several clients were having their hair dyed with different types of hair dyes. In order to test the sensitivity of the sensor to ammonia, the QAPT was placed both above the clients head (at the height of the hairdresser's face) and at the height of the clients face. This moment can be seen in red and in grey in Figure 38, respectively, for the use of a permanent hair dye with ammonia. It not only shows that the QAPT is sensible to variations in ammonia concentration but also that the ammonia concentrations to which the hairdressers are exposed are extremely high, being much higher than the range of the MQ137 sensor (the sensor had an output of

$440\ ppm$ but its range is only from $5\ to\ 200\ ppm$, as such the values above 200 ppm were limited to 200 as they had no scientific value). On the other side, the ammonia concentration levels at which the clients are exposed is much lower, still reaching $20\ ppm$.

Later in the monitorization experiment, in order to test the QAPT's ability with other types of products, the same procedure described above was repeated for a permanent dye without ammonia. This moment is depicted in green and dark orange, for the measurements above the head of the client and at the height of its face, respectively. In these measurements, the QAPT still reacted but at a much smaller scale (around $20\ ppm\ max$.) than with the permanent dye with ammonia. Another visible difference is that both measurements did not differ with the change in height, contrariwise to the measurements with the other dye. These differences might come from the lack of selectiveness of the MQ137 sensor, which might have indicated the attenuated presence of ammonia, measuring instead alcohol or another component that replaces the ammonia in the ammonia-free product.

Continuing the experiment, the QAPT AQS was placed in another room of the hair salon in order to test the whole area of the scenario being studied. In this room, as can be seen in Figure 38, the ammonia concentration was lower, of around $6\ ppm$ of ammonia, which was expected as there were no clients dyeing their hair in this area. Surprisingly, after some time in this room, the QAPT suddenly turned on its red light and measured ammonia concentrations well beyond its range, as seen in orange in Figure 38. This was later found to be caused by the use of permanent oil in one of the client's hair. The hairdresser confirmed that that product was one of the most active and ammonia-rich products she had and the client denoted that every time she did this process she had rashes on the scalp, which is consistent with one of the symptoms of high exposure to ammonia, particularly in people with sensitive skin.

Continuing the monitorization, one of the hairdressers used hairspray in a client, which again led the sensor to measure a peak of ammonia concentration well above its range, as seen in blue in Figure 38. This was an example of a false positive because the components of the hairspray did not include ammonia but included alcohol as a solvent, which triggered the MQ137 sensor.

Lastly, QAPT also sensed the use of a product with a small concentration of ammonia, that reached a peak of approximately $45\ ppm$ of ammonia, much lower than the other products with high amounts of ammonia. Leaving the hair salon, the measured ammonia concentration fell back to values below the measuring range of the MQ137 sensor, as was expected.

This performance trial allowed to verify that the concentrations of ammonia in a hair salon can be quite high, affecting the indoor air quality. This can be particularly harmful to the hairdressers that are subject to these concentrations in high amounts and for long periods of time. The mean concentration of ammonia, without encompassing the measurements of specific products that lead to peaks in the acquired data, was of $8.25\ ppm$. This value is in accordance with the literature, as the average ammonia concentration in 50 studied hair salons was of $2.3\ ppm$ with the Portuguese reference value being of $20\ ppm$ [45]. The value acquired with the QAPT AQS is higher than the $2.3\ ppm$ but it can be explained, as the hairs salons might not have three clients dyeing their hair at the same time, as occurred in this study. Even so, the mean value acquired is between the Portuguese reference and the values stated in [45].

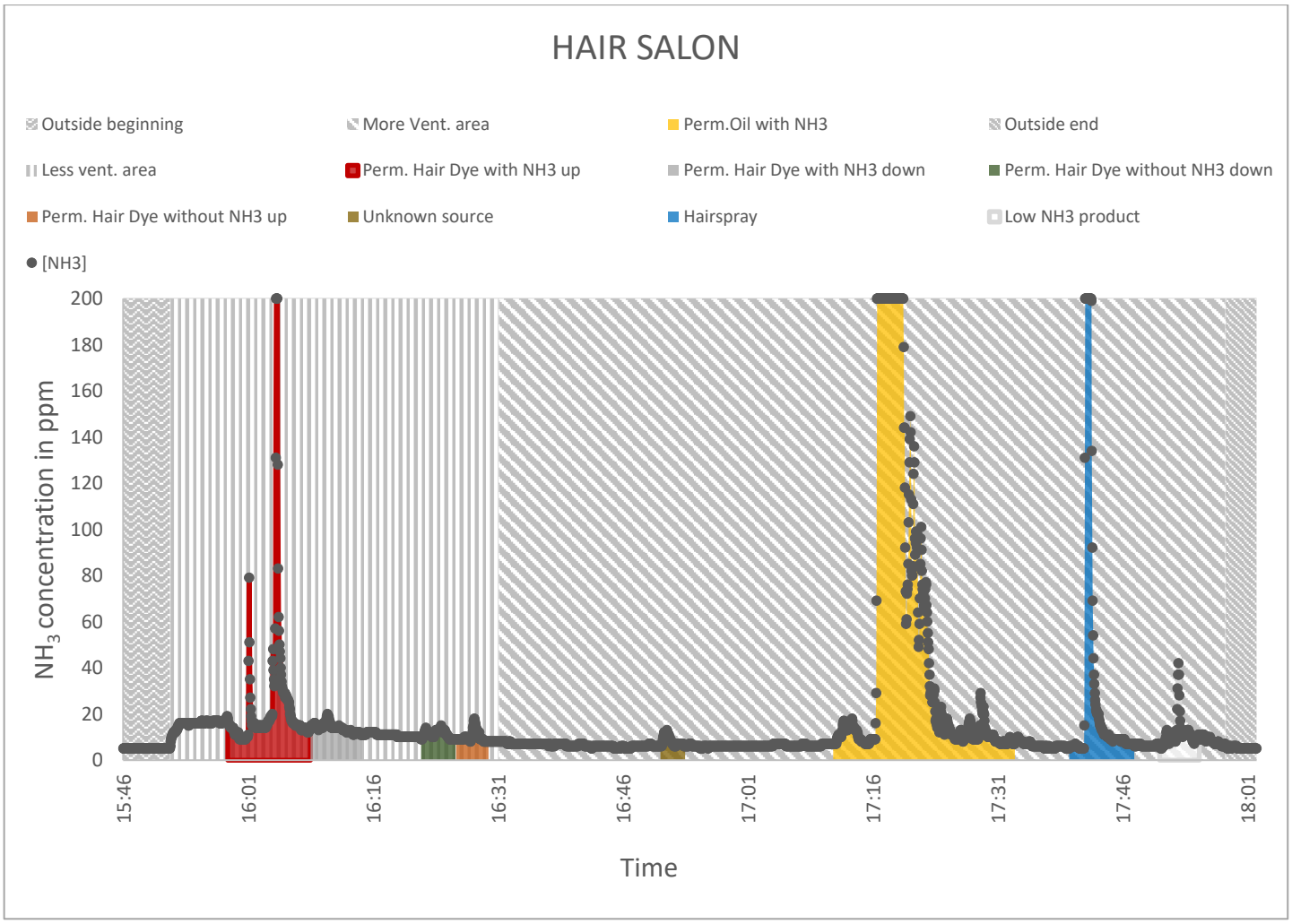

Figure 38 - Performance trial 3: Hair Salon ammonia concentration

4.6.4. Poultry Farm

In the fourth and last performance trial, the QAPT AQS was tested on a poultry farm. This farm held approximately 14000 poults, which occupied the same beds for four weeks. As can be seen in Figure 39, the measurements indicated a rise in ammonia concentration as soon as it was taken inside the poultry farm warehouse, reaching values above 10 ppm. The monitorization was conducted by walking around the perimeter of the warehouse. In Figure 39 one can observe, in green, that the proximity to the windows affected the concentrations of ammonia in the warehouse, diminishing the values to 5 ppm in the immediately adjacent areas. Going to the middle corridor of the warehouse, the ammonia concentrations significantly rose, as seen in yellow, particularly in the areas directly in front of the ventilators, depicted in orange. This situation was due to the ventilator's work, that pulled the air behind them, concentrating it in the area in front, inherently increasing the ammonia concentrations in these areas. At the end of the monitorization, it was possible to observe that the outside air around the warehouse still had traces of ammonia, coming from the interior of the warehouse. The measured concentration diminished with the increase in distance from the warehouse, as expected, reaching values below the measuring range of the QAPT at a distance of approximately 5 m.

The average concentration of ammonia inside the poultry farm warehouse was of 12 ppm, which is in accordance with the literature, as this value is between 5 and 18 ppm [46]. This validates the measurements from the QAPT monitorization even though it could not have the ammonia sensor calibrated in relation to a reference sensor.

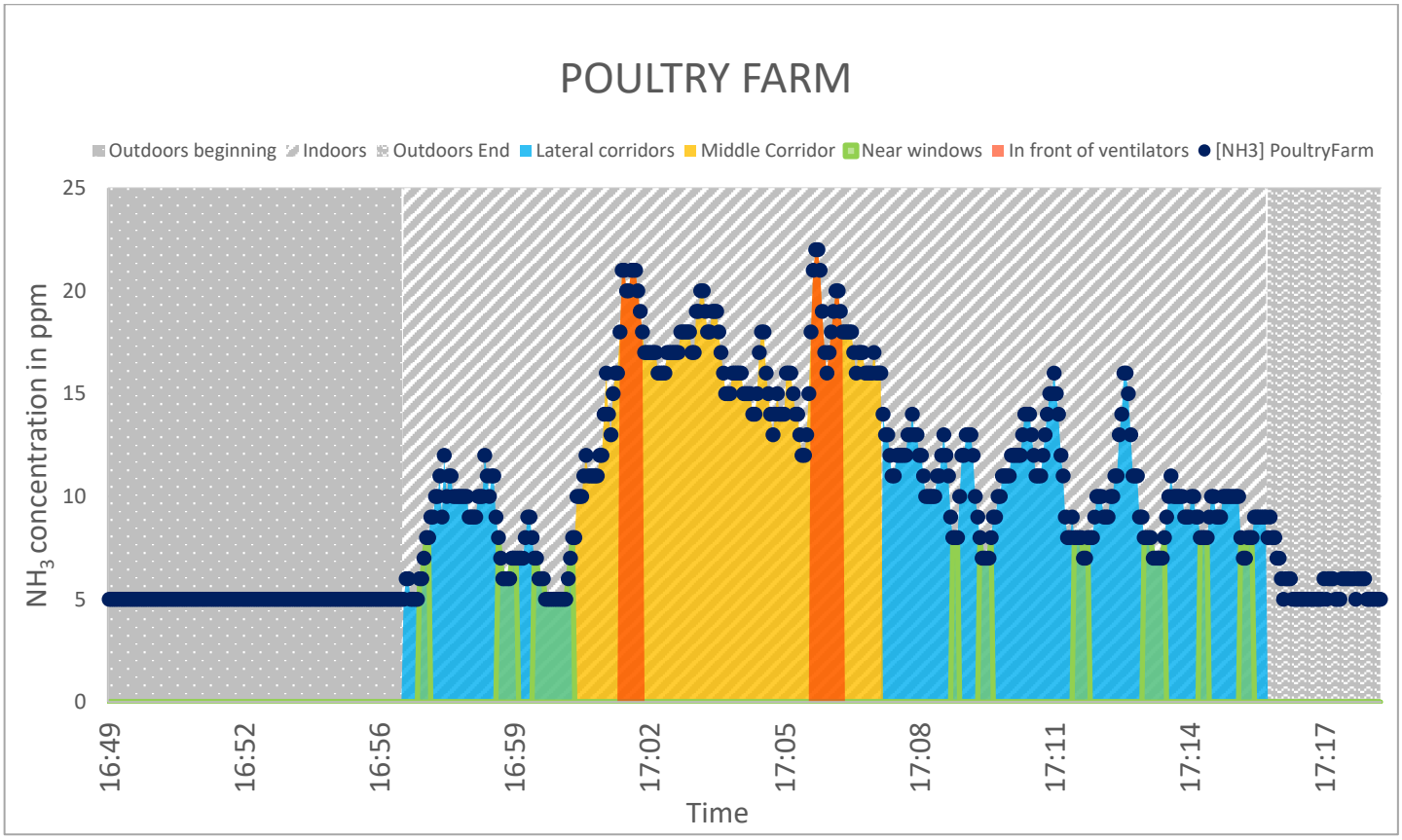

Figure 39 - Performance trial 4: Poultry farm ammonia concentration

5. Conclusions, Recommendations and Further Work

The main question of this dissertation had come upon the viability and validity of a low-cost air quality station for indoor and outdoor air quality. This question was verified with the performance tests to the hair salon and poultry farm, with ammonia values being in accordance with the available literature for both scenarios, even without calibration with a reference sensor. The QAPT also allowed to shed some light on the long-term harmful air-quality conditions some hair salon professionals are subjected to, as they were exposed to values much higher than the limits presented in Table 2.1 (above 200 ppm).

The thermographic analysis was important to pinpoint the heat sources in the interior of the QAPT and understand the impact of the choice of power supply, proving that the power bank was the best choice. It also reiterated the importance of the separation of the air sampling system.

The best sensor for secondary data of temperature and humidity seems to be the BME280 because it was the sensor that presented the most similar behaviour in relation to the reference sensor and had the smaller dispersion, measuring additional variables that the other sensors did not (pressure, approximate altitude).

This allowed for a better performance of the low-cost sensor analysed, the MQ137, which had its sensibility to both parameters highly diminish upon calibration, as intended. This improvement is also benefic for its low-cost application to other sensors.

As expected, the low-cost sensor used in the QAPT had selectivity issues, that were demonstrated in the performance trials (particularly in the two first trials). These issues can be a challenge to the low-cost air quality stations but have already been addressed in other studies.

The air sampling system created for the QAPT can have a good applicability in further studies on the subject of low-cost air quality stations, as it solves some of the common problems: diminishes the thermal impact of the electronics, does not corrupt the samples with lubricants from fans and other devices and improves the response time of the station. This system allows the sensors to measure outside/ambient air and be placed inside a case being, therefore, less affected by air movement in moving monitorization (particularly if, in future studies, the control of the diaphragm pump's voltage is done in order to assure isokinetism).

In terms of the power systems utilised, the solar power bank was the most interesting option, not only because of its "green" potential but also because of its capacity and small effect in terms of circuit heating. One possible addition to the power bank and batteries is the use of a CJMCU-LTC3588 Energy Harvester Breakout Module, that costs about 6€ and is a very promising new piece of technology for the application in small devices. This module, if installed, can increase the energy autonomy of the system (which is of 28h), resorting to the piezoelectric effect and actively micro-charging the station.

The communication to the cloud was not achieved during the course of this work. However, this was achieved in other similar works with success, a fact that proves its potential application to this system [39]. Although not achieved, the studies conducted during the course of this work allowed to point to an apparently good choice for the application of the communications: the Raspberry Pi, that has more memory (particularly important if the system is to be of increased complexity with more sensors), wifi and Bluetooth connection, amongst other further capabilities. However, this connection is not advised in the current form of the QAPT system as it would undermine its portability due to the large increase in energy consumption.

The QAPT AQS was made with the expansion to the monitorization of more air pollutants in mind, particularly from the low-cost MQ sensors family. As such, the code is easily applicable to other sensors of this family with the respective alterations according to the type of sensor. The case was designed to be able to hold more sensors, with a lateral interior space that can be quickly used to maximise the QAPT's air quality monitoring capabilities with the addition of other sensors.

The developed air quality station is, as intended, economically viable, either in its current arrangement (135€) or with the eventual improvement of capabilities, with connection to Wi-Fi and data logging to the cloud (best option: alternative 1 – 165€). In terms of practical viability, the system has been proven to work well on both static and moving monitorization, and its construction is easily replicable.

This thesis also initiated a path in data visualisation, not only with a LED and LCD to inform the user of its air condition without the need to access an external device but also with the representation of data in QGIS. This representation allowed for a much better spatial interpretation of the data and might be increasingly interesting with the eventual application on a network of low-cost air quality portable stations.

6. References

[1] K. C. London, "London Air," 2019. [Online]. Available: https://www.londonair.org.uk/LondonAir/guide/LondonHistory.aspx. [Consulted in 12 02 2019].

[2] R. Wu, X. Song, D. Chen, L. Zhong, X. Huang, Y. Bai, W. Hu, S. Ye, H. Xu, B. Feng, T. Wang, Y. Zhu, J. Fang, S. Liu, J. Chen, X. Wang, Y. Zhang e W. Huang, "Health benefit of air quality improvement in Guangzhou, China: Results from a long time-series analysis (2006–2016)," *Environment International,* vol. 126, pp. 552-559, 2019.

[3] T. P. R. o. C. Ministry of Environmental Protection, "2012 Report on the State of the Environment in China," 2012.

[4] K. Dong, R. Sun, H. Jiang e X. Zeng, "CO2 emissions, economic growth, and the environmental Kuznets curve in China: What roles can nuclear energy and renewable energy play?," *Journal of Cleaner Production,* vol. 196, pp. 51-63, 2018.

[5] W. H. Organization, "Ambient Air Pollution: a global assessment of exposure and burden of disease," WHO Document Production Services, Geneva, Switzerland, 2016.

[6] V. Sass, N. Kravitz-Wirtz, S. M.Karceski, A. Hajat, K. Crowder e D. Takeuchi, "The effects of air pollution on individual psychological distress," *Health & Place,* vol. 48, pp. 72-79, 2017.

[7] J. Lelieveld, K. Klingmüller, A. Pozzer, U. Pöschl, M. Fnais, A. Daiber e T. Münzel, "Cardiovascular disease burden from ambient air pollution in Europe reassessed using novel hazard ratio functions," *European Heart Journal,* vol. ehz135, 2019.

[8] E. E. Agency, "EEA Signals 2013 - Every breath we take: Improving air quality in Europe," Publications Office of the European Union, Copenhagen, 2013.

[9] C. o. T. N. R. C. Committee on Acute Exposure Guideline Levels, "Acute Exposure Guideline Levels for Selected Airborne Chemicals: Volume 6," The Nacional Academies Press, Wasshington, D.C., 2007.

[10] L. Y. M. R. Kwak Dongwook, "Ammonia gas sensors: A comprehensive review," *Talanta,* vol. 204, pp. 713-730, 2019.

[11] S.V.Krupa, "Effects of atmospheric ammonia (NH3) on terrestrial vegetation:a review," *Environmental Pollution,* vol. 124, pp. 179-221, 2003.

[12] L. W. Z. R. H. Z. J. X. Meng Zhaoyang, "Summertime ambient ammonia and its effects on ammonium aerosol in urban Beijing, China," *Science of the Total Environment,* vol. 579, pp. 1521-1530, 2016.

[13] H. S. Ferm Martin, "Trends in atmodpheric ammonia and particulate ammonium concentrations in Sweden and its causes," *Atmospheric Environment,* vol. 61, pp. 30-39, 2012.

[14] E. E. Agency, "Air Quality in Europe - 2018 report," EEA, 2018.

[15] F. J. M. H. M. A. B. C. A. J. Morán Marta, "Ammonia agriculture emissions:From EMEP to a high resolution inventory," *Atmospheric Pollution Research* , vol. 7, pp. 786-798, 2016.

[16] Y. X. L. Y. L. H. Y. X. C. J. G. W. Y. Z. Wang Ruyu, "Characteristic of atmospheric ammonia and its relationship with vehicle emissions in a megacity in China," *Atmospheric Environment,* pp. 97-104, 2018.

[17] V. M. K. A. C. M. A. A. A. B. A. R. M. L.-M. P. B.-H. G. R. S. M. d. l. C. A. F.-C. R. .. Reche Cristina, "Urban NH3 levels and sources in six major Spanish cities," *Chemosphere,* vol. 119, pp. 769-777, 2014.

[18] A. A. B. J. M. V. Q. M. M. Backes Anna, "Ammonia emissions in Europe, part II: How ammonia emission abatement strategies affect secondary aerosols," *Atmospheric Environment,* vol. 126, pp. 153-161, 2015.

[19] "delta15N of lichens reflects the isotopic signature of ammonia source," *Science of the Total Environment,* vol. 653, pp. 698-704, 2018.

[20] Hanwei Electronics Co., Ltd, "MQ-137 GAS SENSOR - TECHNICAL DATA".

[21] D. Technologies, "CleanSpace Tag," 2019. [Online]. Available: https://our.clean.space/. [Consulted in 1 2 2019].

[22] N. Inc., "AtmoTube: About," NotAnotherOne Inc., 2019. [Online]. Available: https://atmotube.com/. [Consulted in 01 02 2019].

[23] D. GmbH, "decentlab," Decentlab GmbH, [Online]. Available: https://www.decentlab.com/#home. [Consulted in 01 02 2019].

[24] apambiente, "QualAr: Base de Dados Online sobre a Qualidade de Ar," apambiente, [Online]. Available: https://qualar.apambiente.pt/qualar/index.php. [Consulted in 02 02 2019].

[25] E. E. Agency, "European Air Quality Index," European Environment Agency, 19 09 2019. [Online]. Available: https://airindex.eea.europa.eu/. [Consulted in 19 09 2019].

[26] Sandra Moreira, APA, Departamento de Políticas e Estratégias de Ambiente, "Procedimentos regionais de informação e alerta no âmbito da qualidade do ar: Relatório de Ambiente e Saúde," 2010.

[27] C. d. O. d. D. Regionais, "A Região de Lisboa e Vale do Tejo em Números," 2009.

[28] IPMA, "PLANO DE ATIVIDADES: PROJETAR A INVESTIGAÇÃO CIENTÍFICA PARA RESPONDER AO DESAFIO DO SÉCULO XXI -VIVER BEM DENTRO DOS LIMITES DO PLANETA," 2017.

[29] B. Doyle, T. Cummins, C. Augustenborg e J. Aherne, "Report No.193: Ambient Atmospheric Ammonia in Ireland, 2013-2014," Environmental Protection Agency, County Wexford, Ireland, 2017.

[30] CCAC, "Ammonia Standards".

[31] The National Institute for Occupational Safety and Health (NIOSH), “Ammonia,” 28 September 2011. [Online]. Available: https://www.cdc.gov/niosh/pel88/7664-41.html. [Consulted in 20 September 2019].

[32] T. Bjorn e v. d. B. A. Olthuis Wouter, “Ammonia sensors and their applications—a review,” *Sensors and Actuators B - chemical,* vol. 107, pp. 666-667, 2004.

[33] ElectronicsTutorials, “Thermistors,” AspenCore, 2017. [Online]. Available: https://www.electronics-tutorials.ws/io/thermistors.html. [Consulted in 12 Junho 2019].

[34] R. AG, “The Capacitive Humidity Sensor,” Rotronic AG, [Online]. Available: https://www.rotronic.com/en/humidity_measurement-feuchtemessung-mesure_de_l_humidite/capacitive-sensors-technical-notes-mr. [Consulted in 14 Junho 2019].

[35] Idealvac, “Vacuum Pumps - Dry Diaphragm”.

[36] Zhengzhou Winsen Electronics Technology Co., Ltd, “Ammonia Gas Sensor (Model: MQ137) Manual, Version 1.4,” 2015.

[37] Adafruit, “Adafruit TCA9548A 1-to-8 I2C Multiplexer Breakout,” lady ada , 11 September 2015. [Online]. Available: https://learn.adafruit.com/adafruit-tca9548a-1-to-8-i2c-multiplexer-breakout/wiring-and-test. [Consulted in 10 December 2018].

[38] D. Workshop, “Using a Real Time Clock with Arduino,” DroneBot Workshop, 2019. [Online]. Available: https://dronebotworkshop.com/real-time-clock-arduino/. [Consulted in 16 11 2018].

[39] A. R. Soares, “Desenvolvimento e teste de um protótipo móvel com sensores low cost,” *UNIVERSIDADE DE LISBOA, FACULDADE DE CIÊNCIAS, DEPARTAMENTO DE ENGENHARIA GEOGRÁFICA, GEOFÍSICA E ENERGIA,* 2018.

[40] P. Stoffregen, “ DS1307RTC/examples/SetTime/SetTime.ino,” 10 March 2016. [Online]. Available: https://github.com/PaulStoffregen/DS1307RTC/blob/master/examples/SetTime/SetTime.ino. [Consulted in 15 April 2019].

[41] Aosong Guangzhou Electronics Co., Ltd., “Temperature and Humidity Module: DHT11 Product Manual”.

[42] Aosong Electronics Co.,Ltd, “Digital-output relative humidity & temperature sensor/module: DHT22 (DHT22 also named as AM2302)”.

[43] Bosch Sensortec, “BME280 - data sheet: Combined humidity and pressure sensor,” 2018.

[44] N. I. f. O. S. a. Health, “NIOSH Pocket Guide to Chemical Hazards/Ammonia,” National Institute for Occupational Safety and Health, 29 November 2018. [Online]. Available: https://www.cdc.gov/niosh/npg/npgd0028.html. [Consulted in 01 September 2019].

[45] R. E. H. R M Harrison, Indoor Air Pollution, Royal Society of Chemistry, 2019.

[46] P. W. G. G. Koerkamp, J. H. M. Metz, G. H. Uenk, V. R. Phillips, M. R. Holden, R. W. Sneath, J. L. Short, R. P. White, J. Hartung, J. Seedorf, M. Schroder, K. H. Linkert, S. Pedersen, H. Takai,

J. O. Johnsen e C. M.Wathes, “Concentrations and Emissions of Ammonia in Livestock Buildings in Northern Europe,” *J. agric. Engng Res.,* vol. 70, pp. 79-95, 5 January 1998.

[47] L. Xiau, C. Sitian, L. Hong, H. Sha, Z. Daqiang e N. Huansheng, “A Survey on Gas Sensing Technology,” *Sensors,* vol. I2, pp. 9635-9665, 2012.

Annexe A - QAPT's Code

A.1. R0 Finder

```
//Code to Calculate R0

void setup() {
Serial.begin(9600);
}

void loop() {
float sensor_volt;
float RS_air; //sensor resistance
float R0; //Unknown R0
float sensorValue=0;
for(int x = 0 ; x < 500 ; x++) //loop
{
sensorValue = sensorValue + analogRead(A3); //Add analog values of sensor 500
times
}
sensorValue = sensorValue/500.0; //Average of the readings
sensor_volt = sensorValue*(5.0/1023.0); //Transform to voltage
RS_air = ((5.0*10.0)/sensor_volt)-10.0; //Calculate RS for 0 ammonia amb
R0 = RS_air/(3.6); //Calculate R0

//Display values in serial
Serial.print("R0 = ");
Serial.println(R0);
Serial.print("Rs_AIR = ");
Serial.println(RS_air);
delay(1000); //Wait a second
}
```

A.2. Read Time

```
// Code to read time from Tiny RTC with I2C multiplexer


#include <Wire.h>
#include <TimeLib.h>
#include <DS1307RTC.h>
#define TCAADDR 0x70

////////////////////////////////////////////////////////////////

void tcaselect(uint8_t i) {
if (i > 7) return;

Wire.beginTransmission(TCAADDR);
Wire.write(1 << i);
Wire.endTransmission();
}



////////////////////////////////////////////////////////////////


void setup() {
Serial.begin(9600);
while (!Serial) ; // wait for serial
delay(200);
Serial.println("DS1307RTC Read Test");
Serial.println("-------------------");
}

void loop() {
tcaselect(7);

tmElements_t tm;

if (RTC.read(tm)) {
Serial.print("Ok, Time = ");
print2digits(tm.Hour);
Serial.write(':');
print2digits(tm.Minute);
Serial.write(':');
print2digits(tm.Second);
Serial.print(", Date (D/M/Y) = ");
Serial.print(tm.Day);
Serial.write('/');
Serial.print(tm.Month);
Serial.write('/');
Serial.print(tmYearToCalendar(tm.Year));
Serial.println();
} else {
if (RTC.chipPresent()) {
Serial.println("The DS1307 is stopped.  Please run the SetTime");
Serial.println("example to initialize the time and begin running.");
Serial.println();
} else {
```

```
Serial.println("DS1307 read error!  Please check the circuitry.");
Serial.println();
}
delay(9000);
}
delay(1000);
}

void print2digits(int number) {
if (number >= 0 && number < 10) {
Serial.write('0');
}
Serial.print(number);
}
```

A.3. Set Time

```
//  Code to set time from Tiny RTC with I2C multiplexer

#include <Wire.h>
#include <TimeLib.h>
#include <DS1307RTC.h>
#define TCAADDR 0x70

const char *monthName[12] = {
"Jan", "Feb", "Mar", "Apr", "May", "Jun",
"Jul", "Aug", "Sep", "Oct", "Nov", "Dec"
};

tmElements_t tm;

////////////////////////////////////////////////////////////////

void tcaselect(uint8_t i) {
if (i > 7) return;

Wire.beginTransmission(TCAADDR);
Wire.write(1 << i);
Wire.endTransmission();
}



////////////////////////////////////////////////////////////////

void setup() {

tcaselect(7);
bool parse=false;
bool config=false;

// get the date and time the compiler was run
if (getDate(__DATE__) && getTime(__TIME__)) {
parse = true;
// and configure the RTC with this info
if (RTC.write(tm)) {
config = true;
}
}

Serial.begin(9600);
while (!Serial) ; // wait for Arduino Serial Monitor
delay(200);
if (parse && config) {
Serial.print("DS1307 configured Time=");
Serial.print(__TIME__);
Serial.print(", Date=");
Serial.println(__DATE__);
} else if (parse) {
Serial.println("DS1307 Communication Error :-{");
Serial.println("Please check your circuitry");
} else {
Serial.print("Could not parse info from the compiler, Time=\"");
Serial.print(__TIME__);
Serial.print("\", Date=\"");
```

```
Serial.print(__DATE__);
Serial.println("\"");
}
}

void loop() {
}

bool getTime(const char *str)
{
tcaselect(7);
int Hour, Min, Sec;

if (sscanf(str, "%d:%d:%d", &Hour, &Min, &Sec) != 3) return false;
tm.Hour = Hour;
tm.Minute = Min;
tm.Second = Sec;
return true;
}

bool getDate(const char *str)
{
tcaselect(7);
char Month[12];
int Day, Year;
uint8_t monthIndex;

if (sscanf(str, "%s %d %d", Month, &Day, &Year) != 3) return false;
for (monthIndex = 0; monthIndex < 12; monthIndex++) {
if (strcmp(Month, monthName[monthIndex]) == 0) break;
}
if (monthIndex >= 12) return false;
tm.Day = Day;
tm.Month = monthIndex + 1;
tm.Year = CalendarYrToTm(Year);
return true;
}
```

A.4. Main Code

```
//////////////////////////

//Code for the QAPT prototype

//Made by Ana Antunes

//Faculty of Sciences of the University of Lisbon - 2019

#include <SD.h>
#include <SPI.h>
#include <Wire.h>
#include <math.h>
#include <TimeLib.h>
#include <DS1307RTC.h>
#include <Adafruit_Sensor.h>
#include <Adafruit_BME280.h>
#include <LiquidCrystal_I2C.h>


#define SEALEVELPRESSURE_HPA (1013.25)
#define TCAADDR 0x70

//assign a unique id to the bme sensor and RTC:
Adafruit_BME280 bme1;
tmElements_t tm;

//to communicate with the SD card
const int chipSelect = 4;

//counter for datalogging:
int nr = 1;

//file to log data:
File dataFile;

//// Set the LCD I2C address
LiquidCrystal_I2C lcd(0x27, 2, 1, 0, 4, 5, 6, 7, 3, POSITIVE);

//Set RGB LED pins
int redpin = 2; //select the pin for the red LED
int bluepin = 3; // select the pin for the  blue LED
int greenpin = 7; // select the pin for the green LED
int val;

//Counter and array for storage of 3 NH3 values
int i=0;
int mySensValsNH3[3];
int mySensValsh1[3];
int mySensValst1[3];
int mySensValsAlt1[3];
int NH3mean=0;
int h1mean=0;
int t1mean=0;
int Alt1mean=0;
int ppmNH3calibrround;
int sumNH3=0;
int sumh1=0;
int sumt1=0;
int sumAlt1=0;
```

```
////////////////////////////////////////////////////////////////
// TCA9548A I2C multiplexer function:
void tcaselect(uint8_t i) {
if (i > 7) return;

Wire.beginTransmission(TCAADDR);
Wire.write(1 << i);
Wire.endTransmission();
}

////////////////////////////////////////////////////////////////////


void setup() {

Serial.begin(9600);
lcd.begin(16, 2);
pinMode(redpin, OUTPUT);
pinMode(bluepin, OUTPUT);
pinMode(greenpin, OUTPUT);

Serial.print("Initializing SD card...");
// see if the card is present and can be initialized:
if (!SD.begin(chipSelect)) {
Serial.println("Card failed, or not present");
// don't do anything else:
while (1);
}
Serial.println("card initialized.");

File dataFile = SD.open("datalog1.csv", FILE_WRITE);
if (dataFile) {
dataFile.println(" , , , , , , "); //line to separate datasets
String Header = "Date, Time, RH[%], T[oC], Height[m], [NH3]";
dataFile.println(Header);
dataFile.close();
Serial.println(Header);
} else {
Serial.println("Couldn't open log file");
}




//initialize the BME280 sensor:
tcaselect(4);
if (!bme1.begin(0x76)) {
/* There was a problem detecting the bme1 ... check your connections */
Serial.println("Ooops, no bme1 detected ... Check your wiring!");
}

//Heating time...
Serial.println("Please wait...Preparing system.");

//write to LCD:
tcaselect(2);
///set the cursor to (0,0):
lcd.setCursor(0,0);
lcd.print("Please wait...");
```

```
/// set the cursor to (16,1):
lcd.setCursor(0,1);
lcd.print("Preparing system");
delay(900000); //Heating time of the MQ137 resistance
Serial.println("Ready!!!");
lcd.setCursor(0,0);
lcd.print("Ready!!!        ");
lcd.setCursor(0,1);
lcd.print("                ");
}



////////////////////////////////////////////////////////////////

void loop() {

const int MQ137_PIN = A3;
const float RL_MQ137 = 1.0;    // kohm (FC-22 module = 1.0 kohm)
const float CLEAN_AIR_RATIO_MQ137 = 3.6;    // Taken from datasheet graph
float sensorValue_MQ137;
float sensor_volt_MQ137;
float Rs_MQ137;    // kohm
const float R0_MQ137 = 16.10;  // kohm , from the R0 finder sketch
float AirFraction_MQ137;
float AirFractionMin_MQ137 = 0.118851;
float AirFractionMax_MQ137 = 0.388153;
float AirFractionCurva33_MQ137;
float AirFractionCurva85_MQ137;
float AirFractionCalibr_MQ137;


//Calculating Rs from analog data
sensorValue_MQ137 = analogRead(A3);
sensor_volt_MQ137 = sensorValue_MQ137*(5.0/1023.0); //Convert to voltage
Rs_MQ137 = ((5.0*RL_MQ137)/sensor_volt_MQ137)-RL_MQ137; //Calculate Rs
AirFraction_MQ137 = Rs_MQ137/R0_MQ137;






//Get RTC date and time:
tcaselect(7);
RTC.read(tm);
int Day = tm.Day;
int Month = tm.Month;
int Year = tmYearToCalendar(tm.Year);
int Hour = tm.Hour;
int Minute = tm.Minute;
int Second = tm.Second;

//Get BME280 sensor data
tcaselect(4);
float h1 = bme1.readHumidity()+6.89;
int h1round = h1;
float t1 = bme1.readTemperature()+0.55;
int t1round = t1;
float Alt1 = bme1.readAltitude(1013.25)+45;
int Alt1round = Alt1;
```

```
float ppmNH3calibr;
float ppmNH3;

//  Calibration of MQ137 considering Temperature and relative humidity based
on Hanwen datasheet, using polinomial regression
AirFractionCurva33_MQ137 = 0.0003 * pow(t1, 2) - 0.0255 * t1 + 1.4004;
AirFractionCurva85_MQ137 = 0.0003 * pow(t1, 2) - 0.0231 * t1 + 1.2808;

if (h1 >= 0 && h1 < 59) {
AirFractionCalibr_MQ137 = AirFraction_MQ137 / AirFractionCurva33_MQ137;
}
else {
AirFractionCalibr_MQ137 = AirFraction_MQ137 / AirFractionCurva85_MQ137;
}



/// Convertion to ppm of NH3:

float expoente_MQ137 = 1 / (-0.257);
ppmNH3 = pow((AirFraction_MQ137 / 0.587), expoente_MQ137);
ppmNH3calibr = pow((AirFractionCalibr_MQ137 / 0.587), expoente_MQ137);

//round [NH3] to an int and then put the values of [NH3], RH and T in the
respective arrays:
for (i=0; i<=2;i=i+1){
ppmNH3calibrround=round(ppmNH3calibr);
mySensValsNH3[i]=ppmNH3calibrround;
sumNH3=sumNH3+mySensValsNH3[i];
mySensValsh1[i]=h1round;
sumh1=sumh1+mySensValsh1[i];
mySensValst1[i]=t1round;
sumt1=sumt1+mySensValst1[i];
mySensValsAlt1[i]=Alt1round;
sumAlt1=sumAlt1+mySensValsAlt1[i];
if(i==2){
//mean of the 3 last values measured
NH3mean=sumNH3/3;
h1mean=sumh1/3;
t1mean=sumt1/3;
Alt1mean=sumAlt1/3;
tcaselect(2);
lcd.setCursor(0,0);
lcd.print("T:");
lcd.print(t1mean);
lcd.print("oC   ");
lcd.print("RH:");
lcd.print(h1mean);
lcd.print("% ");
lcd.setCursor(0,1);
lcd.print("NH3:");
lcd.print(NH3mean);
lcd.print("ppm        ");
}

// Change the colour of the RGB LED according to [NH3]
if (NH3mean >= 5 && NH3mean <= 200) {



if (NH3mean <= 25) {
```

```
analogWrite(greenpin, 150);
analogWrite(bluepin, 0);
analogWrite(redpin, 0);
} else {
if (NH3mean <= 80) {
analogWrite(bluepin, 150);
analogWrite(greenpin, 0);
analogWrite(redpin, 0);
} else {
analogWrite(redpin, 150);
analogWrite(greenpin, 0);
analogWrite(bluepin, 0);
}
}

} else {


if (NH3mean < 5) {
lcd.setCursor(0,1);
lcd.print("[NH3] OutOfRange");
analogWrite(greenpin, 150);
analogWrite(redpin, 0);
analogWrite(bluepin, 0);
} else {
lcd.setCursor(0,1);
lcd.print("[NH3] OutOfRange");
analogWrite(redpin, 150);
analogWrite(greenpin, 0);
analogWrite(bluepin, 0);
}
}

delay(1000);
}

//create strings
String dataString1 = String(Day) + "/" + String(Month) + "/" + String(Year)
+ "," + String(Hour) + ":" + String(Minute) + ":" + String(Second) + ",";
String  dataString2  =  String(h1mean)  +  ","  +  String(t1mean)  +  ","  +
String(Alt1mean) + "," + String(NH3mean);

// open file (only one at a time)so you have to close this one before opening
another
File dataFile1 = SD.open("datalog1.csv", FILE_WRITE);

// if the file is available, write to it:
if (dataFile1) {
dataFile1.print(dataString1);
dataFile1.println(dataString2);
dataFile1.close();


}
// if the file isn't open, pop up an error:
else {
Serial.println("error opening datalog1.csv");
}

Serial.print(dataString1);
Serial.print(dataString2);
```

```
Serial.println();
Serial.println();
Serial.println();



//reset the values for the next loop
i=-1;
sumNH3=0;
sumh1=0;
sumt1=0;
sumAlt1=0;
}
```

A.5. Temperature and Humidity Sensors Test Code

```
#include <SD.h>
#include "DHT.h"
#include <SPI.h>
#include <Wire.h>
#include <TimeLib.h>
#include <DS1307RTC.h>
#include <Adafruit_Sensor.h>
#include <Adafruit_BME280.h>


#define SEALEVELPRESSURE_HPA (1013.25)
#define TCAADDR 0x70

//assign a unique id to each bme sensor and RTC:
Adafruit_BME280 bme1;
Adafruit_BME280 bme2;
tmElements_t tm;


const int chipSelect = 4;

//defining which arduino pins are used to receive the dht sensors data:
#define DHT1PIN 3     //  digital pin for the DHT11_1
#define DHT2PIN 5     //  digital pin for the DHT11_2
#define DHT3PIN 6     //  digital pin for the DHT22_1
#define DHT4PIN 7     //  digital pin for the DHT22_2
//defining the type of dht sensors being used:
#define DHT1TYPE DHT11   // DHT 11_1
#define DHT2TYPE DHT11   // DHT 11_2
#define DHT3TYPE DHT22   // DHT 22_1
#define DHT4TYPE DHT22   // DHT 22_2
//assigning the names, pins and type of each dht sensor:
DHT dht1(DHT1PIN, DHT1TYPE);
DHT dht2(DHT2PIN, DHT2TYPE);
DHT dht3(DHT3PIN, DHT3TYPE);
DHT dht4(DHT4PIN, DHT4TYPE);

int nr = 1;

File dataFile;


////////////////////////////////////////////////////////////
// I2C multiplexer function:
void tcaselect(uint8_t i) {
if (i > 7) return;

Wire.beginTransmission(TCAADDR);
Wire.write(1 << i);
Wire.endTransmission();
}
```

```
////////////////////////////////////////////////////////////////

void setup() {

Serial.begin(9600);

Serial.print("Initializing SD card...");

// see if the card is present and can be initialized:
if (!SD.begin(chipSelect)) {
Serial.println("Card failed, or not present");
// don't do anything else:
while (1);
}
Serial.println("card initialized.");



//initialize the first bme280:
tcaselect(7);
if (!bme1.begin(0x76)) {
/* There was a problem detecting the bme1 ... check your connections */
Serial.println("Ooops, no bme1 detected ... Check your wiring!");
}
//initialize the second bme280:
tcaselect(4);
if (!bme2.begin(0x76)) {
/* There was a problem detecting the bme1 ... check your connections */
Serial.println("Ooops, no bme2 detected ... Check your wiring!");
}

//initiate dht sensors and check if they are working:
dht1.begin();
dht2.begin();
dht3.begin();
dht4.begin();


}
////////////////////////////////////////////////////////////////////////

void loop() {
Serial.println("Inside loop");

tcaselect(2);
RTC.read(tm);

int Day = tm.Day;
int Month = tm.Month;
int Year = tmYearToCalendar(tm.Year);
int Hour = tm.Hour;
int Minute = tm.Minute;
int Second = tm.Second;


tcaselect(7);
int h5 = bme1.readHumidity()*100;
int t5 = bme1.readTemperature()*100;
```

```
tcaselect(4);
int h6 = bme2.readHumidity()*100;
int t6 = bme2.readTemperature()*100;



//creating the variables to read T(C), RH(%), P(hPa) and Alt(m):
float h1 = dht1.readHumidity();
float t1 = dht1.readTemperature(); // Read dht11_1
float h2 = dht2.readHumidity();
float t2 = dht2.readTemperature();  // Read dht11_2
float h3 = dht3.readHumidity();
float t3 = dht3.readTemperature();  // Read dht22_1
float h4 = dht4.readHumidity();
float t4 = dht4.readTemperature();  // Read dht22_2



//create string
String dataString1 = String(Day) + "/" + String(Month) + "/" + String(Year)
+ "," + String(Hour) + ":" + String(Minute) + ":" + String(Second) + ",";
String                                dataString2                                =
String(h1)+","+String(t1)+","+String(h2)+","+String(t2)+",";
String                                dataString3                                =
String(h3)+","+String(t3)+","+String(h4)+","+String(t4);
String                                dataString4                                =
String(h5)+","+String(t5)+","+String(h6)+","+String(t6);

// open the file. note that only one file can be open at a time,
// so you have to close this one before opening another.
File dataFile1 = SD.open("datalog1.csv", FILE_WRITE);

// if the file is available, write to it:
if (dataFile1) {
dataFile1.print(dataString1);
dataFile1.print(dataString2);
dataFile1.println(dataString3);
dataFile1.close();


}
// if the file isn't open, pop up an error:
else {
Serial.println("error opening datalog1.csv");
}

delay(1000);

File dataFile2 = SD.open("datalog2.csv", FILE_WRITE);

// if the file is available, write to it:
if (dataFile2) {
dataFile2.print(dataString1);
dataFile2.println(dataString4);
dataFile2.close();

}
//   if the file doesn t open, pop up an error:
else {
Serial.println("error opening datalog2.csv");
```

```
}

delay(57500);



}
```

Annexe B · Thesis Flowchart

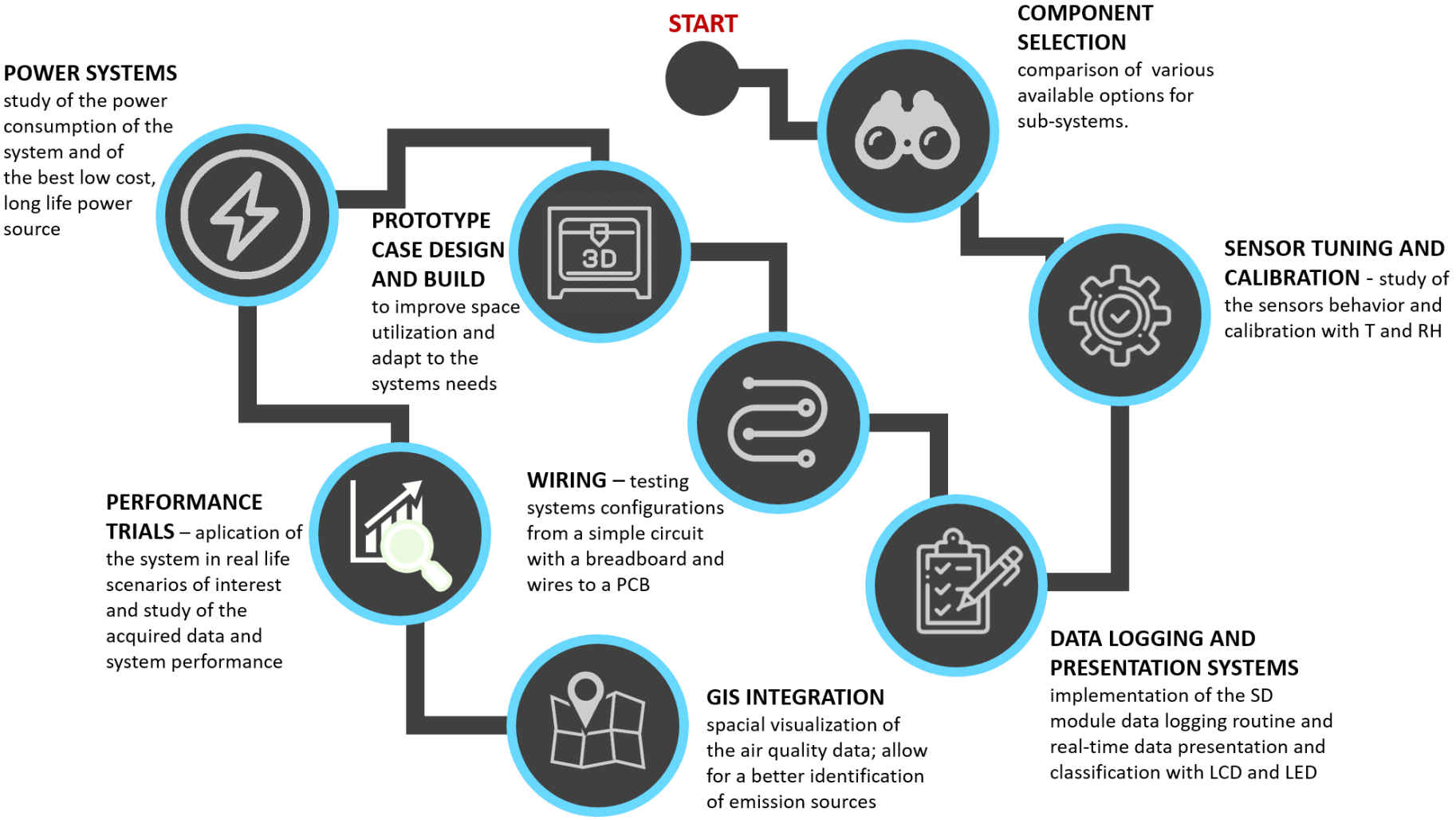

Annexe C· 3D Case Studies

Annexe D · Thermography reports

QAPT POWERED BY USB CONNECTION

Measurements

$B \times 1$	30.8℃
$B \times 2$	29.2℃
Average	26.9℃

Parameters

Emissivity	0.96
Temp.refl.	20℃

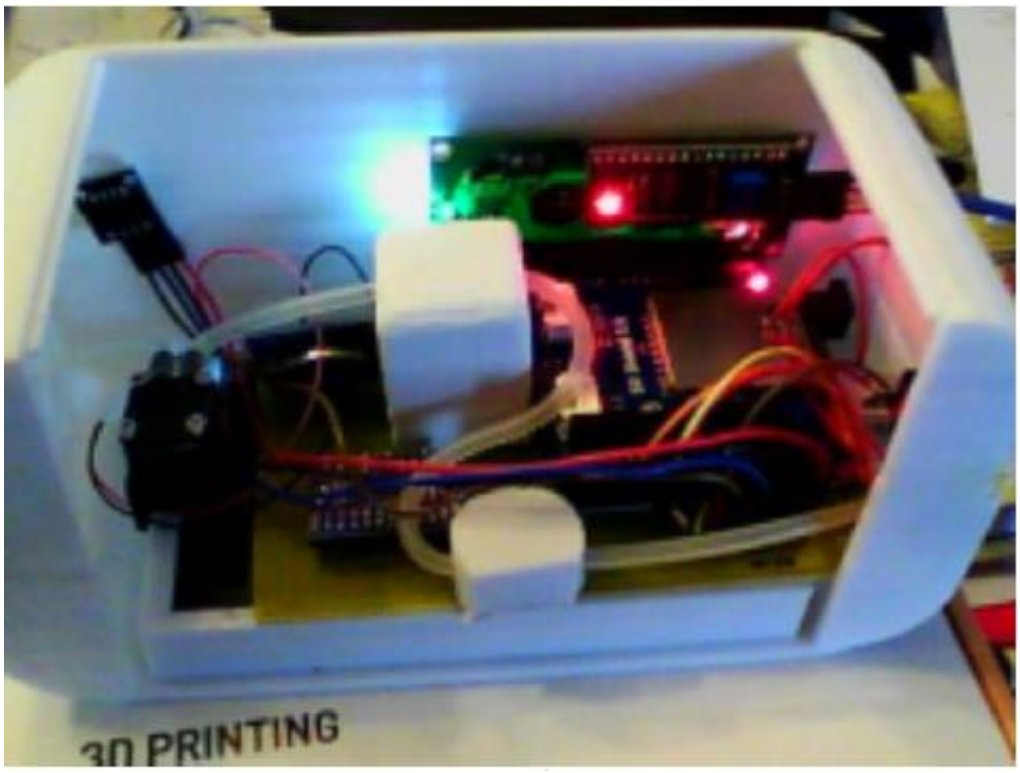

QAPT POWERED BY BATTERY PACK

Measurements

$B \times 1$	42.5℃
$B \times 2$	48.7℃
Average	34.9℃

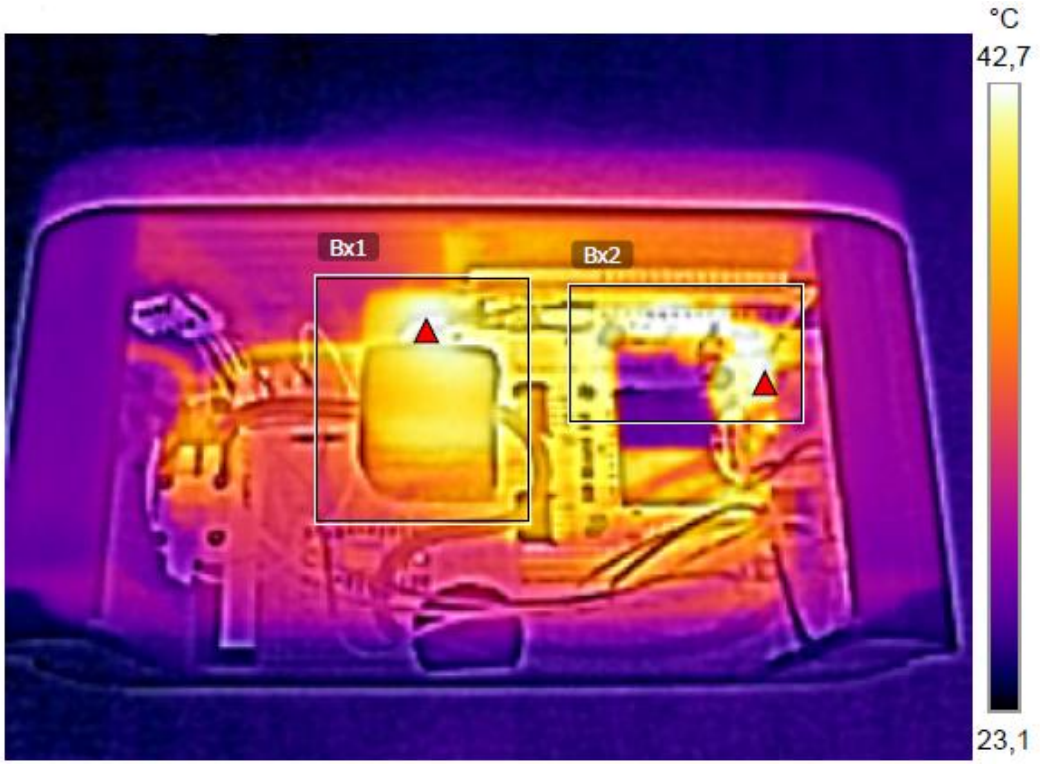

Parameters

Emissivity	0.96
Temp.refl.	20℃